

8-AN

THE PRESSURE BEHAVIOR OF A SHUT-IN WELL DUE TO THE
UPWARD MIGRATION OF A GAS KICK

A thesis

Submitted to the Graduate Faculty of the
Louisiana State University and
Agricultural and Mechanical College
in partial fulfillment of the
requirements for the degree of
Master of Science

in

The Department of Petroleum Engineering

by
Peter G. McFadden
B.S., University of Rhode Island, 1982
December 1984

ACKNOWLEDGEMENTS

The author wishes to extend his deepest thanks to Dr. Adam T. Bourgoyne, Jr., Professor of Petroleum Engineering at Louisiana State University, under whose guidance and supervision this work was completed.

Special thanks are also due to Dr. Zaki Bassionni, Dr. William Holden, and Dr. Julius Langlinais for their timely help and suggestions.

The author also greatly appreciates the help of Jim Sykora and Allen Kelly at the LSU research and training well.

Finally, the author would like to express special thanks to his father, Peter Sr., for his inspiration to pursue a career in engineering. And to his mother, Kathleen Crafton, without whose love and financial support, the author's graduate education would not have been possible.

This research was supported in part by the U.S. Geological Survey, Department of the Interior, under USGS Contract No. 14-08-0001-21169.

TABLE OF CONTENTS

	page
ACKNOWLEDGEMENT	ii
LIST OF TABLES	iv
LIST OF FIGURES	v
ABSTRACT	vii
 <u>Chapter</u>	
I. INTRODUCTION	1
II. BUBBLE SLIP VELOCITY	12
Introduction to Chapter 2	12
Fluid and Gas Densities	21
Effect of Viscosity	22
Effect of Surface Tension	26
Effect of Contamination by Solids	27
Bubble Swarm Velocity	29
Adaptation To Computer Model	31
III. VERTICAL GAS DISTRIBUTION	34
Bubble Size Distribution	34
Entrance Conditions	35
Bubble Stability	37
Reconglomeration	43
IV. DEVELOPMENT OF COMPUTER MODEL	47
V. EXPERIMENTAL PROCEDURES	59
VI. RESULTS	65
VII. CONCLUSIONS	81
VIII. RECOMMENDATIONS	83
 BIBLIOGRAPHY	 86
VITA	88

LIST OF TABLES

<u>Table</u>	<u>page</u>
1. Summary of liquid properties	25
2. Bubble shapes as a function of Reynolds number . . .	26
3. Velocity equations and regions of applicability . . .	32
4. Modifying coefficients	33
5. Equations used in computer model	33
6. Computer time requirements	51
7. Flow Chart: Main Program	53
8. Additional parts of flow chart.	57
9. Average mud properties for the 1984 experiment . . .	64

LIST OF FIGURES

<u>Figure</u>		<u>page</u>
1.	Depth vs pore and fracture pressures for a normally pressured gulf coast well	5
2.	Depth vs pore and fracture pressures for an abnormally pressured gulf coast well	6
3.	Typical backpressure curve	7
4.	Comparison of actual and predicted back pressure curves	9
5.	Terminal velocity of air bubbles in filtered water as a function of req	14
6.	Terminal velocity of air bubbles in tap water as a function of req	15
7.	Typical curve of the terminal velocity of bubbles in filtered water as a function of bubble size	17
8.	Oblate spheroid bubbles	20
9.	Spherical cap bubbles	20
10.	Force balance on a travelling bubble	21
11.	Terminal velocities of air bubbles in various liquids	24
12.	Ratio of swarm velocity to single bubble velocity, as a function of swarm gas fraction . .	30
13.	Typical number and sizes of product bubbles produced during bubble breakup	41
14.	One form of bubble breakup	42
15.	Mechanism by which a small bubble combines with a spherical cap bubble	44

16.	Typical exchange of gas between spherical cap bubbles	45
17.	Example of the initial distribution of a gas kick in the LSU research and training well . . .	49
18.	Subsurface configuration of the LSU research and training well	60
19.	Nitrogen injection at the bottom of the LSU research and training well	62
20.	Gel strength vs time for the 1984 experiment	64
21.	Pressure vs time for the 1982 experiment. Solid line is computer generated data, dotted line is experimental data	66
22.	Approximate average bubble size distribution of the gas kick for the 1982 experiment	67
23.	Pressure vs time for the 1984 experiment. Solid line is computer generated data, dotted line is experimental data	68
24.	Approximate average bubble size distribution of the gas kick in the 1984 experiment	69
25.	Gas flow(scf/min) and mud flow(gpm) out of the well, and surface choke and bottom hole pressures, all vs time	71
26.	Computer generated gas distribution history for the 1982 experiment	74
27.	Computer generated gas distribution history for the 1984 experiment	80

ABSTRACT

The control of high pressure formation fluids while drilling for hydrocarbons is one of the more expensive and potentially dangerous problems of the petroleum industry. Well control is especially difficult when the formation fluid is gas. In the unfortunate circumstance of gas entering the wellbore, the gas or gas kick, as it is called, must be circulated out of the well. Current well control simulators assume that the gas enters the wellbore as a continuous slug, and moves up as a slug during circulation at the same velocity as the drilling fluid. This is known to be inaccurate.

The current study investigates the effects of gas zone elongation and the upward migration of the gas relative to the drilling fluid on the pressure behavior of a well. To isolate the above influences, a static, shut-in well is modeled.

The first step of the current study was to write a computer program that predicts the pressure response of a shut-in offshore well that has taken a gas kick. A flow geometry that is representative of a floating drilling vessel was assumed. Having done this, actual experiments were done at

the Louisiana State University research and training well. The LSU well hydraulically models an offshore drilling platform in 3000 ft. of water that has drilled through 3000 ft. of sediments. The experiments involved pumping a simulated gas kick into the bottom of the LSU well. Surface and bottom hole pressures were recorded as the gas migrated to the surface.

Much was learned about the various factors that control the rate of upward gas migration in a shut-in well. The approximate bubble size distribution of the gas kick was inferred by comparing computer generated pressure profiles with experimental pressure profiles.

Chapter I
INTRODUCTION

As shallow onshore reserves of petroleum become depleted, the oil industry is forced to search in more inaccessible areas, and at much greater depths. Drilling costs increase dramatically under these conditions. These increased costs, together with the responsibility of maintaining environmental quality, have stressed the need for good well control procedures. Improper well control can lead to a surface blowout, probably the single worst catastrophe possible while drilling for or producing hydrocarbons. A surface blowout is the uncontrolled flow of reservoir fluids from the well. This can involve loss of life, loss of the drilling rig, loss of oil and gas, reservoir damage, and environmental damage which can be severe offshore.

A blowout first becomes possible when reservoir fluids enter the wellbore due to insufficient wellbore pressure, caused by;

1. Insufficient mud weight
2. Drilling into an unexpected overpressured porous and permeable formation
3. A level of mud in the hole that is too low

4. Tripping out of the hole too fast causing a swabbing effect.

An influx of reservoir fluids into the wellbore is called a kick. Kick fluids can consist of water, oil, gas, or any combination of the three. The present study focuses on gas kicks only.

A kick can develop into a blowout for any of the following reasons;

1. Equipment failure
2. Inadequate equipment
3. Improper equipment installation
4. Failure of the drill crew to detect the kick early enough
5. Improper drill crew control action.

The oil industry spends hundreds of millions of dollars a year fighting surface blowouts. Much money is also lost from loss of oil and gas revenues.

A more common problem in the oil industry is underground blowouts. This is the uncontrolled flow of reservoir fluids from one formation to another. Although not as dangerous as a surface blowout, underground blowouts are still very ex-

pensive because reserves are lost and often the well has to be redrilled. A properly handled kick taken with sufficient casing set in place will generally not develop into a blow-out.

Specifically, a gas kick occurs when the pressure in the wellbore falls below the pressure in a gas-bearing porous and permeable formation at the same depth. At this point gas starts flowing into the wellbore. If the rig is drilling, the crew should notice the kick by an increase in the mud flow coming out of the well. This is indicated by an increase in the mud level in the pit, which is part of the circulation system. The drilling crew immediately activates the BOP (blowout preventer), sealing off the annular space between the drill pipe and the casing. The top of the drill pipe is also sealed, either by poppet valves in the mud pump or by an inside blowout preventer valve. The fact that the kick is gas can be seen from the difference in casing and drill pipe pressure. The casing pressure will be greater due to the loss of hydrostatic head from mud being displaced from the annulus. The drill pipe pressure will enable calculation of the new kill weight mud needed to offset the pressure in the kicking formation.

Before drilling can resume, the gas must be removed from the well. The operations that restore the well to normal are known as well control procedures. The accepted practice

in the petroleum industry is to circulate down the drill pipe and up the annulus through a surface choke, maintaining a bottom hole pressure slightly higher than the formation pressure. If a meaningful drill pipe pressure is available, this is most easily done by maintaining the drill pipe pressure slightly above its initial shut-in value. The surface choke will maintain backpressure while allowing mud to flow out of the well. This backpressure plotted against cumulative circulated mud is known as an annular backpressure curve.

The closed well can be assumed to be a rigid system. By this we assume that the casing will not flex outward, and the mud is incompressible. For a large gas kick, this assumption is accurate to within a few percent. If the well was open at the top, the gas would expand as it was circulated up the annulus, due to loss of hydrostatic head. This expansion, and the resulting loss of pressure from loss of mud in the annulus would allow more gas to come into the well from the kicking formation. This positive feedback scenario would eventually create a surface blowout. Let us now assume that exactly the same amount of mud is bled from the choke as is pumped down the drill pipe. The gas will not be allowed to expand and will carry the formation pressure up with it, resulting in high pressures at all depths in the wellbore. Formation fracture just below the casing will result in an underground blowout. Proper manipulation

of the choke will bring the kick to the surface without any problems. A "window" between formation pore pressure and fracture pressure provides a margin for error. These pressures are plotted versus depth as shown in Figure 1 for an example normally pressured gulf coast well, and in Figure 2 for an example abnormally pressured gulf coast well. The pressures are displayed as the equivalent density of a mud column back to the surface that would exert the actual pressure at any depth.

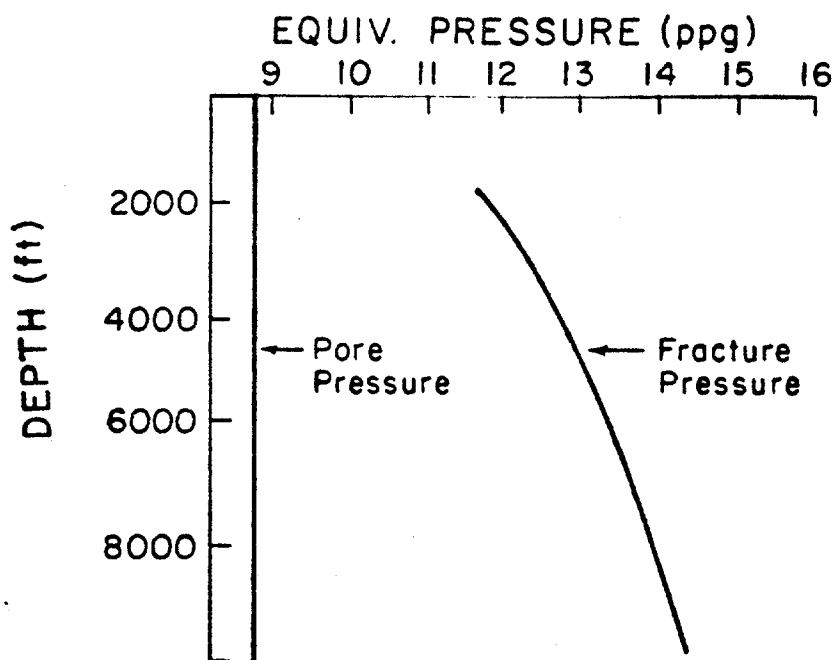


Figure 1: Depth vs pore and fracture pressures for a normally pressured gulf coast well

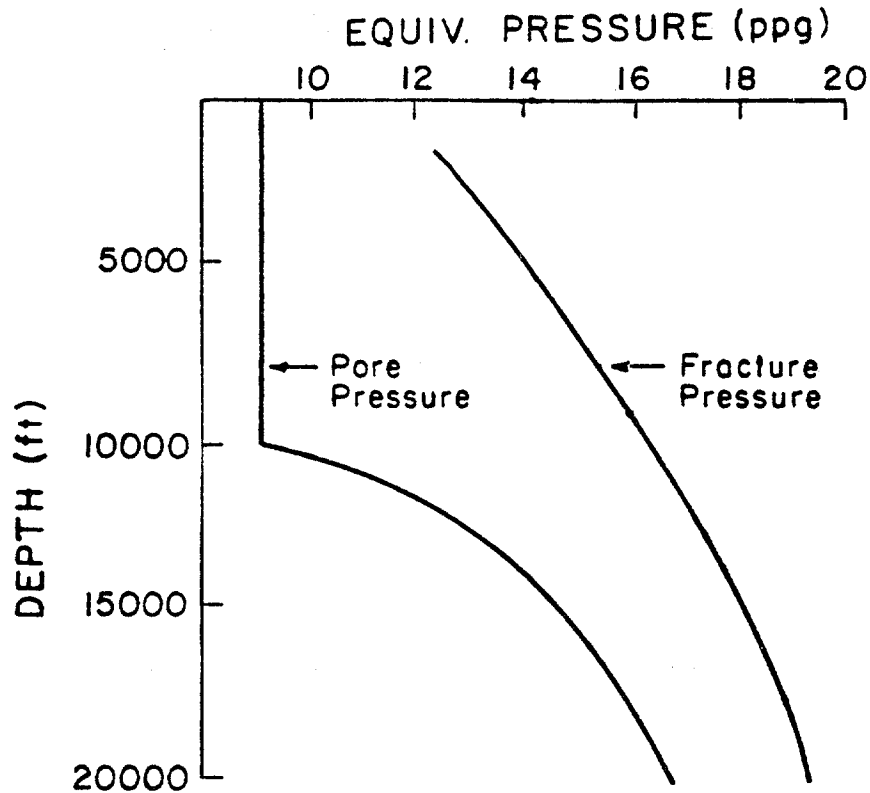


Figure 2: Depth vs pore and fracture pressures for an abnormally pressured gulf coast well

As can be seen from Figure 2, the area between the pore and fracture pressure curves is much smaller in the overpressured horizons in which the oil industry is now forced to search. This can make well control generally more difficult.

A typical backpressure curve for an onshore well pumping out a gas kick is shown in Figure 3.

Modern methods use computer simulations to predict the pressure response of a well during well control operations.

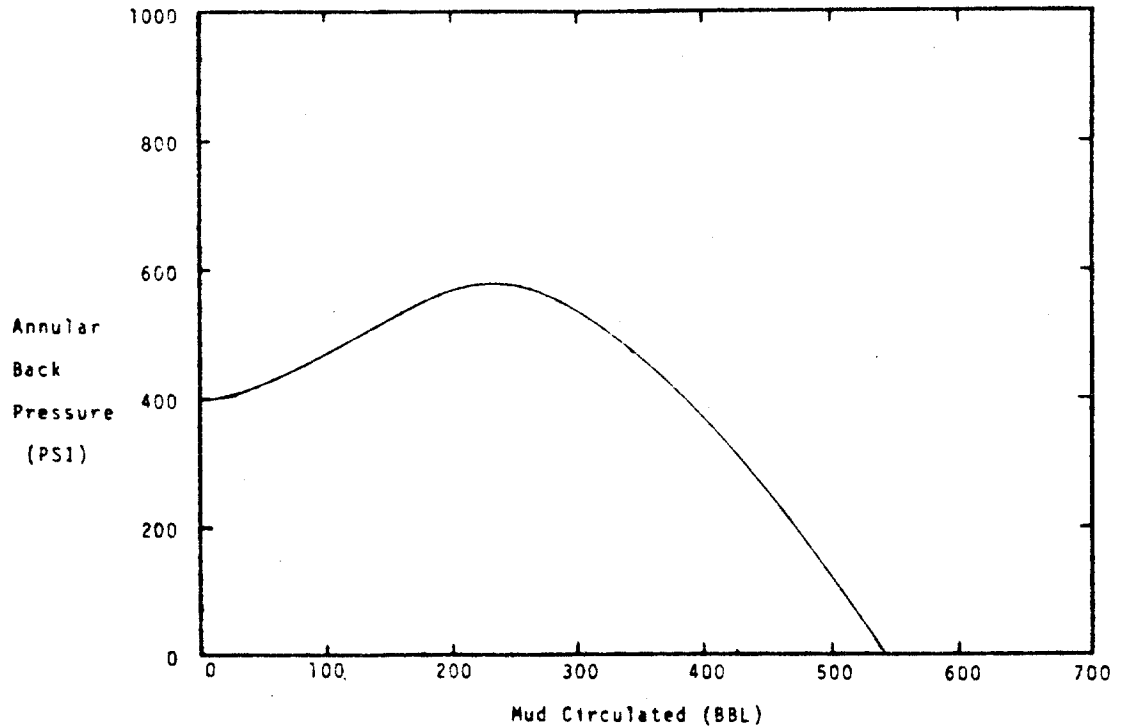


Figure 3: Typical backpressure curve

Computer simulations of well control operations are desirable for a number of reasons. Knowledge of what the maximum casing pressure could be during well control operations before a well is drilled allows an operator to make arrangements for the proper equipment and to develop contingency plans in case a large gas kick is taken. Computer studies allow an operator to evaluate various alternative pressure control procedures. Also, computer simulations of pressure control operations can be carried out on a real time interactive basis in order to train field personnel in the proper procedures for pumping out gas kicks.

Accurate computer simulation of pressure control responses requires an accurate knowledge of gas and liquid behavior in the well. Other researchers at LSU (Mathews, 1980), have shown that some of the assumptions used in modern well control simulations poorly predict the pressure behavior in an actual well when gas is present. The two assumptions found to be the most at fault are: (1) that a gas kick enters the well as a solid continuous slug and remains such during all subsequent well control operations; and (2) that the gas has no slip velocity of its own relative to the mud. In other words, the gas moves at the same velocity as the mud as it is circulated out of the well.

These assumptions are invalid because: (1) as gas enters the wellbore it will have a tendency to mix with the mud already there, forming bubbles; (2) the instability of large bubbles causes them to break up into smaller bubbles; and (3) the buoyancy of the bubbles causes them to move upward through the mud at a significant velocity. These three actions combine with the fact that larger bubbles move upward faster than smaller bubbles to spread the gas-contaminated zone over much larger portion of the well than would be predicted by the assumption above shown to be invalid.

A typical comparison of actual and predicted back pressure curves is shown in Figure 4 (Radar, 1973).

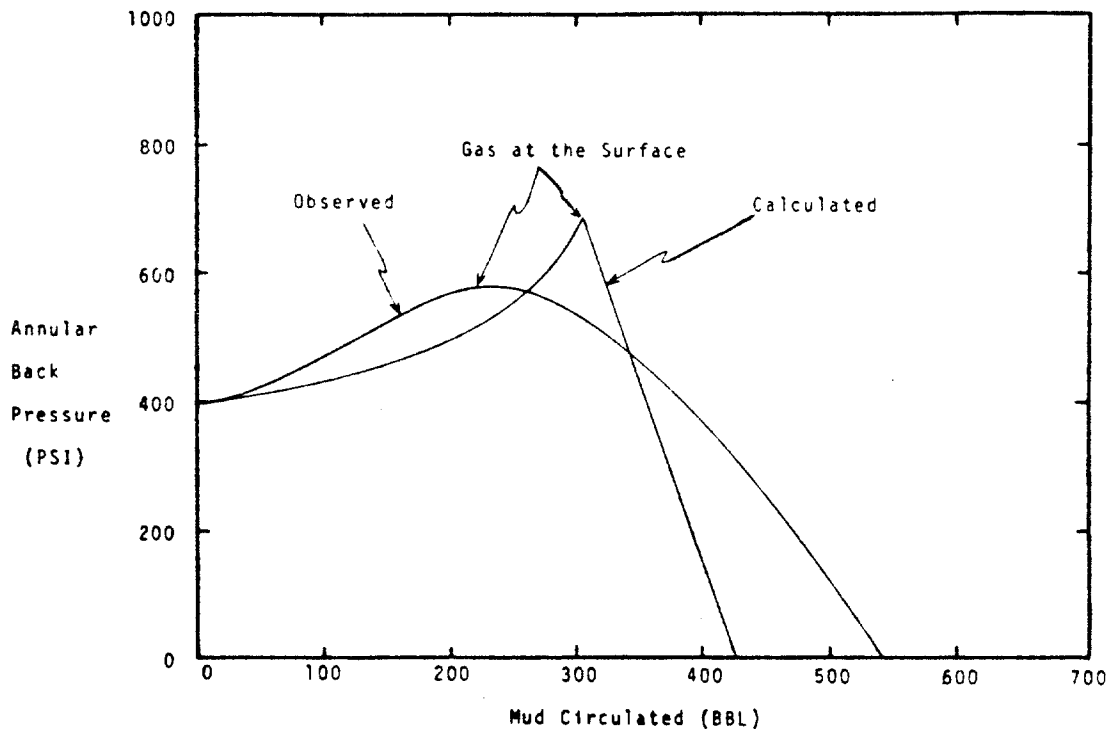


Figure 4: Comparison of actual and predicted back pressure curves

The differences between the curves in Figure 4 are explained by 1, 2, and 3 above. The observed profile is lower and more rounded because the gas is spread out over a large vertical distance. Also, the pressure peak occurs sooner in the observed profile, owing to the velocity of the bubbles relative to the mud.

The main thrust of this study is to determine the influence of (1) bubble stability, (2) bubble slip velocity, and (3) gas contaminated zone elongation on the pressure behavior of a well that has taken a gas kick. A circulating well has many other contributions to the pressure profile. In order to isolate the above three influences, a shut-in, non-

circulating well is studied and modeled. Hopefully, extension to a circulating well will be a part of future research.

This study is being conducted as part of a large ongoing research effort towards the development of improved well control systems for offshore drilling operations. Ultimately, it is hoped that a more accurate understanding of the fluid behavior in a well will lead to an accurate computer simulation of well control operations.

The primary objectives of the current study are;

1. to determine the upward velocity distribution of bubbles formed in a well during a gas kick.
2. to write a computer program that will predict the annular pressure profile of a shut-in offshore well when a gas kick is taken.
3. to experimentally generate annular pressure profiles after having pumped an actual gas kick into a well having a geometry similar to a deep water offshore well.
4. to use kick entrance phenomena and bubble size stability, together with 2 and 3 above, in an attempt to determine an average bubble size distribution as the bubbles migrate up the well.

A previous study at LSU included a computer program modeling a gas kick. The model utilized a single bubble size (Bourgoyne, 1984). The current study is an extension of the previous one in that a distribution of 34 sizes is used. However, the current study is limited in that the bubble size distribution is held constant with time. In an actual gas kick the bubble size distribution may change with time.

Chapter II
BUBBLE SLIP VELOCITY

2.1 INTRODUCTION TO CHAPTER 2

An accurate knowledge of bubble slip velocity is indispensable in the calculation of pressure creep in a shut-in well as a gas kick migrates upward. As was mentioned earlier, the pressure is calculated from the vertical gas distribution. How the vertical gas distribution changes with time is directly related to the slip velocity of the individual bubbles.

Bubble slip velocity is defined as the upward velocity of the bubble relative to the mud. Only the terminal velocity is of interest in this study. At terminal velocity, the drag force is exactly balanced by the buoyant force. A bubble reaches its terminal velocity in a matter of seconds, and it takes hours for it to reach the surface. The terminal velocity will change with time due to changes in bubble size caused by changes in pressure and temperature. However, it is assumed that a bubble always travels at its terminal velocity.

There is a fairly large body of literature on the motion of gas bubbles in liquids. For a number of reasons, most of it is of limited use. The investigations have largely been restricted to bubbles rising in water in nonannular geometries. Many investigations dealt only with a limited range of bubble sizes. Most of the authors did not record the circumstances surrounding their experiments in sufficient detail. Many authors report releasing successive bubbles and averaging the velocities without noting the time increment between bubbles. Residual turbulence from preceding bubbles can increase a bubble's velocity up to 39% (Haberman et al., 1954). Also, many experimenters do not comment upon the purity of their experimental liquids. The following example demonstrates the importance of this. Figure 5 is a plot of bubble velocity as a function of equivalent radius* for filtered water (Haberman et al., 1954). Figure 6 is the same plot for tap water (Ibid). Note the departure of the curves for bubbles of .035 to .28 centimeter equivalent radius. Bubbles having an r_{eq} of .068 centimeter in filtered water travel over 100% faster than the same size bubble in tap water. The minute amount of contaminants in tap water can have a profound effect. The mechanisms of this effect are discussed in the section entitled "Contamination".

* The equivalent radius, r_{eq} , is the radius of a spherical bubble having the same volume as the bubble in question. This definition is necessary because bubbles can deform and become nonspherical.

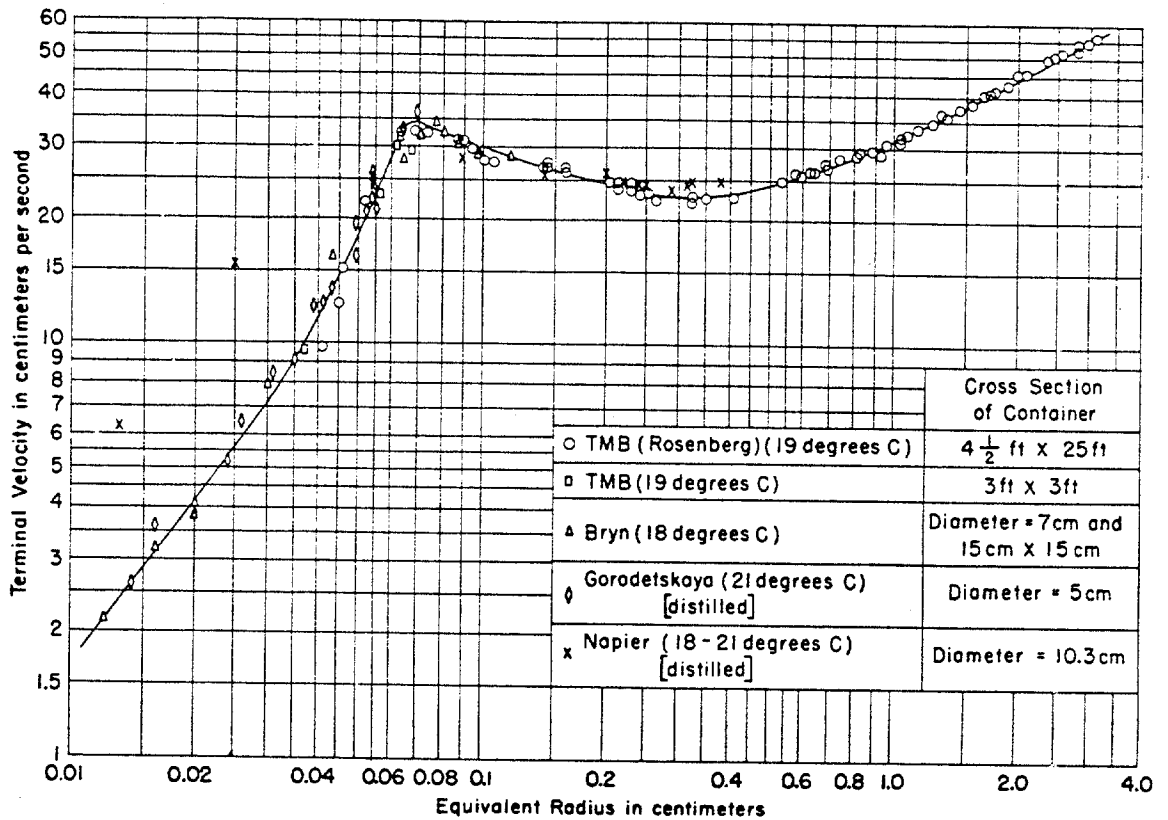


Figure 5: Terminal velocity of air bubbles in filtered water as a function of req

O'Brien and Gosline (1935), plotted the data of various authors for bubbles rising in water. The data was fairly consistent for large bubbles, but wide discrepancies in the data for small and medium size bubbles were found. Note the large discrepancy between the experimenters Napier and Bryn for small bubbles in Figure 5. This can probably be attributed to varying liquid purity, residual turbulence, wall effects from the use of tubes not much larger than the bubble diameter, and errors in the measurement of small bubble

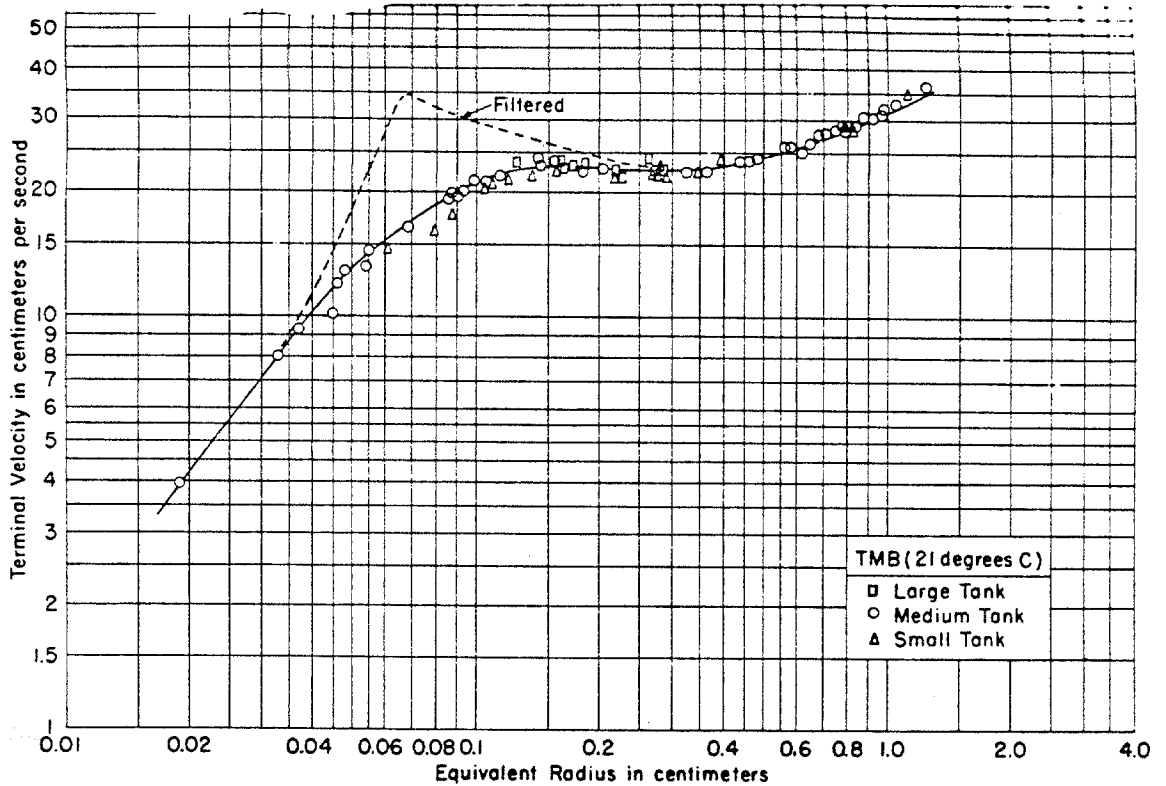


Figure 6: Terminal velocity of air bubbles in tap water as a function of req

sizes. This, together with the limited amount of data for more viscous fluids, and the scarcity of data for contaminated and nonnewtonian fluids made it difficult to model bubble rise velocities in drilling mud. The opacity of drilling mud makes meaningful experiments on the mud itself extremely difficult.

The mechanics of bubble rise velocity are extremely complicated. It involves an intricate balance among gravity

forces, inertial forces, viscous forces, and surface forces. Gravity forces, or buoyant forces, provide the upward driving force on the bubble. Viscous forces tend to retard the motion of small bubbles. Inertial forces give rise to pressure drag or form drag, which retards the motion of larger bubbles, and also acts to deform them. Surface forces result from the intermolecular attraction of the fluid molecules at the gas-liquid interface. There is a tangential tensile force at every point on this surface. This is referred to as surface tension. Surface tension causes the surface to seek the smallest possible area, resulting in a spherical bubble in the absence of other forces.

Many authors have tried to derive equations for bubble-rise velocities from a mechanistic standpoint (Peebles et al., 1953; p. 89). These attempts have largely failed, except for the simplest bubble geometries. Dimensional analysis has also been tried; and this, too, has yielded only limited results (Ibid.). The dimensionless parameters important in the analysis are the Reynolds, Weber, and Froude numbers.* The current author feels that dynamic similarity may not be possible in this analysis. To utilize dynamic

* Reynolds number, $Re = \rho * v * D / \mu$, is a dimensionless ratio of inertial forces on the bubble to viscous forces. Weber number, $We = \rho * v^2 * D / \sigma$, is a dimensionless ratio of inertial forces to surface tension forces. Froude number, $Fr = v / (g * D)^{.5}$, or in fully expanded form, $\rho * v^2 * d^2 / \rho * g * D^3$, is a dimensionless ratio of inertial forces to buoyant forces. ρ - liquid density; v - bubble velocity; D - bubble diameter; μ - liquid viscosity; σ - surface tension; g - gravitational acceleration.

similarity, one would have to be able to match all three dimensionless parameters among various liquids. This is not possible if the liquids have different properties. Various combinations of these parameters have been tried with more promising results (Ibid.; p. 97). Because of the difficulties involved from a theoretical standpoint, the current author felt a better approach would be to empirically model well documented experimental data.

For a clean, low to moderate viscosity fluid, a bubble-rise velocity curve can be divided into four regions of distinct behavior. A curve for pure water is shown in Figure 7 (Mendelson, 1967).

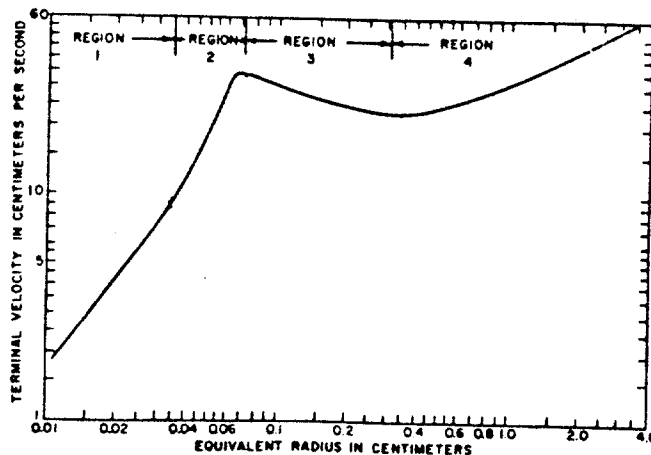


Figure 7: Typical curve of the terminal velocity of bubbles in filtered water as a function of re_q

The characteristic shape of this curve can be explained as follows:

Region 1 - Solid sphere region

$r_{eq} < .035$ cm for water; $Re < 2$;

In this region a bubble behaves as a solid sphere. The bubbles obey Stokes' law, and the velocity is limited by viscous drag.

Region 2 - Fluid sphere region

$.035$ cm $< r_{eq} < .07$ cm for water;

$Re > 2$ up to a value peculiar to individual liquids.

In this region, spherical bubbles traveling in straight-line paths give rise to a velocity greater than that of an equal size solid sphere. The velocity is still limited by viscous drag. However, due to gas circulation within the bubble, shear stresses at the gas-liquid interface are reduced, and the drag is less than that predicted by Stokes' law.

Region 3 - Oblate spheroid region;

$.07$ cm $< r_{eq} < .3$ cm for water.

Re range peculiar to individual liquids.

This region is characterized by a sharp increase in drag. The bubbles are no longer spherical, but

ellipsoidal, flattened in the direction of travel. Deformation increases with Reynolds number. The drag increases due to greater frontal area exposed to the flow. In addition to this, the C_d^* increases. This is caused by quicker flow separation around the more curved ellipsoid. In a moderate to high viscosity liquid, the path is straight up. In low viscosity fluids, vortex shedding gives rise to zig-zagged or spiral motion, and a further increase in drag. Oblate spheroid bubbles are shown in Figure 8.

Region 4 - Spherical cap region

$re_q > .3$ cm for water up to limit of stability.

In this region, the bubble has a spherical cap and a flat or wavy bottom. In a high viscosity liquid, the bottom is almost perfectly flat. Turbulence gives rise to a wavy or oscillating bottom when the bubble is travelling in a low to moderate viscosity liquid. All paths are rectilinear in this region. Spherical cap bubbles are shown in Figure 9.

* Drag coefficient, a dimensionless measure of bubble drag, is defined as $C_d = 2F / \rho v^2 A$. F - drag force on bubble; ρ - liquid density; v - bubble velocity; A - frontal area of bubble exposed to flow. The drag coefficient is a function of Reynolds number and bubble shape. It is independent of liquid density, bubble velocity, and bubble size.



Figure 8: Oblate spheroid bubbles

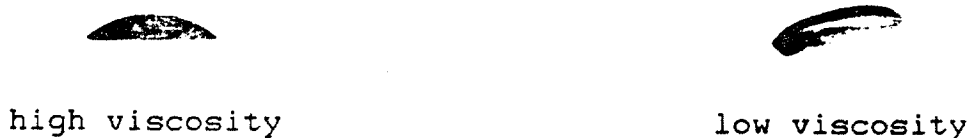


Figure 9: Spherical cap bubbles

Bubble velocity is a function of fluid and gas density, fluid and gas viscosity, surface tension, fluid contamination, and the proximity of walls and other bubbles. The following is a brief explanation of how these properties and conditions influence bubble rise velocities.

2.2 FLUID AND GAS DENSITIES

The buoyancy provided by the difference between fluid and gas densities is the driving force for the upward motion of the bubble. How this affects the velocity of a solid sphere (region 1 bubble) can be shown with Stokes' law. Figure 10 is a force balance on a travelling bubble.

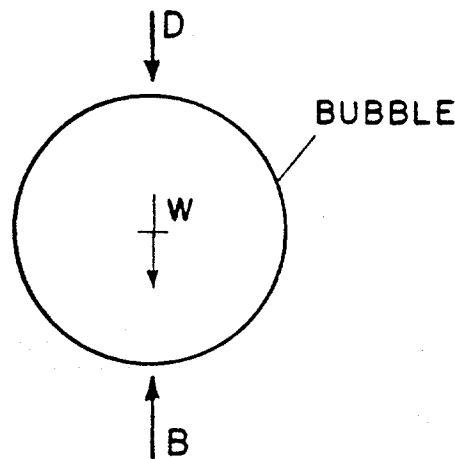


Figure 10: Force balance on a travelling bubble

The weight W of a bubble of gas density ρ_g , and volume V is expressed by:

$$W = \rho_g * V * g \dots \dots \dots (2.1)$$

where g is the acceleration of gravity. The buoyant force B , is the weight of the displaced liquid, given by:

$$B = \rho_l * V * g \dots \dots \dots (2.2)$$

The difference of these is the upward force F on the bubble. In terms of bubble radius this is:

$$F = B - W = (\rho_l - \rho_g) * g * (4/3 * \pi * r^3) \dots \dots \dots (2.3)$$

Stokes' law states that the viscous drag on a sphere traveling at velocity v is:

$$D = 6 * \pi * r * \mu * v \dots \dots \dots (2.4)$$

At terminal velocity, the drag force is exactly balanced by the net sum of the buoyant force and the weight. Setting F equal to D and solving for the velocity yields:

$$v = r^2 * (\rho_l - \rho_g) / (9 * \mu) \dots \dots \dots (2.5)$$

This equation is only valid for region 1. The driving force, defined by Equation (2.3) is valid for any bubble in regions 1-4. However, the drag is an unknown function in regions 2-4, not a simple one as it is for region 1. Experimental data must be used to find general equations for the velocity in regions 2-4.

2.3 EFFECT OF VISCOSITY

How viscosity affects a region 1 bubble is easily seen from Equation (2.5). Velocity is inversely proportional to viscosity in region 1. Velocity is approximately inversely proportional to the square root of viscosity in region 2. Viscosity slows a region 3 bubble only slightly. Region 4

seems totally unaffected by viscosity, except where wall effects are significant. As a bubble travels upward, liquid flows down around the sides of the bubble. In a confined or semi-confined area, this liquid backflow can create additional viscous drag.

Despite the lack of influence of viscosity on bubble velocity in regions 3 and 4, viscosity delays the onset of all regions in all cases. This behavior can be seen in Figure 11 (haberman et al., 1954; p.18). Figure 11 is an experimental plot of bubble-rise velocity as a function of equivalent radius for a number of different liquids. Table 1 gives the properties of the various liquids (Ibid). Hot and cold water display this delay nicely. Transition from region 2 to region 3 occurs at $re_q = .068$ cm for hot water and $re_q = .078$ cm for cold water. Cold water has 2.6 times the viscosity and 10% greater surface tension, both of which are felt to delay region transition. Table 2 lists the Re range of the three major bubble shapes for various liquids (Ibid). A high viscosity fluid can cause the fluid sphere region to disappear. This is because the bubble can deform below a Reynolds number of 2, the Reynolds number above which a fluid sphere develops. For a high viscosity liquid, regions 2 and 3 are replaced by a new transition region between regions 1 and 4. Bubbles in this new region experience increased drag from deformation, but not as a result of turbulence. Mineral oil, with a viscosity of 58 cp, displays this behavior in Figure 11.

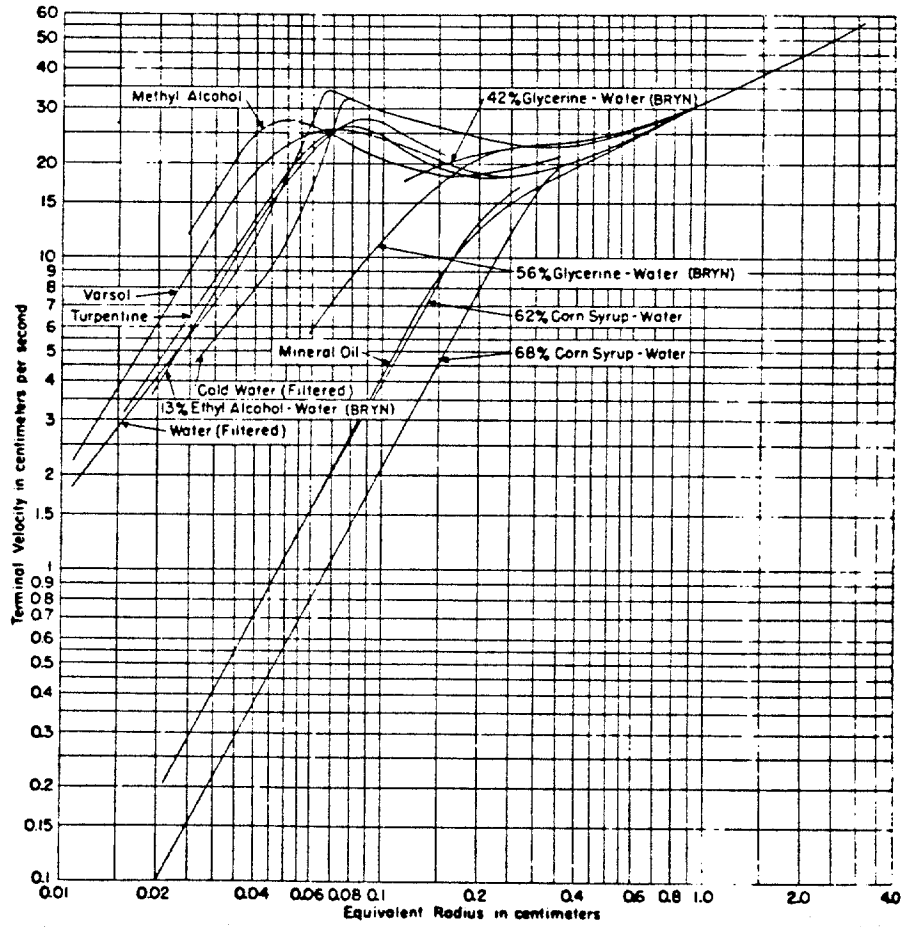


Figure 11: Terminal velocities of air bubbles in various liquids

TABLE 1
Summary of liquid properties

Liquid	Temperature deg C	Viscosity μ poises	Density ρ gm/cc	Surface Tension σ dynes/cm	"M" $\frac{g\mu^4}{\rho\sigma^3}$
Water	19	0.0102	0.998	72.9	0.26×10^{-10}
Water	21	0.0098	0.998	72.6	0.24×10^{-10}
Cold Water	6	0.0147	0.999	74.8	1.08×10^{-10}
Hot Water	49	0.0056	0.989	68.1	0.307×10^{-11}
Glim Solution	19	0.0103	1.000	32.8	2.78×10^{-10}
Mineral Oil	27.5	0.580	0.866	20.7	1.45×10^{-2}
Varsol	28	0.0085	0.782	24.5	4.3×10^{-10}
Turpentine	23	0.0146	0.864	27.8	24.1×10^{-10}
Methyl Alcohol	30	0.0052	0.782	21.8	0.89×10^{-10}
62 percent Corn Syrup and Water	22	0.550	1.262	79.2	0.155×10^{-3}
68 percent Corn Syrup and Water	21	1.090	1.288	79.9	0.212×10^{-2}
56 percent Glycerine and water (Bryn)	18	0.0915	1.143	69.9	1.75×10^{-7}
42 percent Glycerine and water (Bryn)	18	0.043	1.105	71.1	4.18×10^{-8}
13 percent Ethyl Alcohol and water (Bryn)	22	0.0176	0.977	43.5	1.17×10^{-10}
Olive Oil (Arnold)	22	0.73	0.925	34.7	0.716×10^{-2}
Syrup (Bond)	17	180	1.48	91	0.92×10^6

TABLE 2

Bubble shapes as a function of Reynolds number

Liquid	Reynolds Number		
	Spherical	Ellipsoidal	Spherical Cap
Water	less than 400	400 - 5000	larger than 5000
Cold water	275	275 - 3000	3000
Mineral Oil	0.45	0.45 - 80	80
Varsol	80	80 - 2000	2000
Turpentine	85	85 - 1500	1500
Methyl Alcohol	80	80 - 4000	4000
62% Corn Syrup and Water	0.28	0.28 - 60	60
68% Corn Syrup and Water	2.5	2.5 - 110	110

2.4 SURFACE TENSION

Surface tension is an intermolecular attraction that causes there to be a tensile force in the surface at the gas liquid interface. In the absence of other forces, this action causes the surface to seek the smallest area possible, resulting in a sphere. Drag forces try to deform a traveling bubble. Surface forces are dominant for a small bubble resulting in spheres for regions 1 and 2, while inertial forces are dominant for a medium to large size bubble, resulting in deformation in regions 3 and 4. Transition to regions 3 and 4 has to do with shape deformation. Surface tension resists deformation, therefore delaying the onset of

regions 3 and 4. Delay in the transition to region 3 is demonstrated in Figure 11. Liquids with higher surface tensions transfer to region 3 at larger radii.

2.5 EFFECT OF CONTAMINATION BY SOLIDS

Contamination is a much more elusive and hard to quantify influence on bubblerise velocity. It influences the velocity in several indirect ways. As shown earlier in Figures 5 and 6, the minute amounts of contaminants in tap water can have a profound effect on both the velocity of bubbles and the behavior of the different regions. Small amounts of contaminants are sufficient because they tend to congregate and stay on the gas-liquid interface. The contaminants interfere with the intermolecular attraction of the fluid molecules, thereby lowering surface tension. This affects the velocity through shape alteration and changes in region transition. If one could look closely at a contaminated bubble, one would find the front of the bubble relatively free of contaminants. The contaminants tend to congregate on the back end of the bubble. There is a negative contamination gradient towards the front of the bubble. That means there is a positive surface tension gradient in the same direction. The effect of contamination on surface tension, and the influence of a surface tension gradient on deformation resistance and region transition are all extremely difficult to quantify.

Contamination has an adverse effect on region 2 bubble behavior. Recall that region 2 is the fluid sphere, where gas circulation within the bubble reduces the shear stresses at the gas-liquid interface. Foreign particles interfere with the transfer of momentum from the liquid to the gas, retarding the "fluid sphere" effect. This is also hard to quantify.

No experimental research concerning the influence of fluid contamination on bubble velocities could be found by the current author. One paper was found dealing with the influence of contamination from a purely theoretical standpoint (Ishii et al., 1980). However, this research does not predict the difference between the behaviors of tap water and filtered water. This difference is felt to be a shape dependent phenomenon. Only the changes in viscous and form drags resulting from the changes in flow geometry imposed by the conditions of a contaminated surface were investigated. They did not look at the influence of contamination on bubble shape and region transition. They also don't have any experimental evidence to support their findings.

It was difficult to determine the effect of fluid contamination on the rising velocity of a bubble in drilling mud due to the meager amount of literature available. The reason this particular subject is so important is that drilling mud is an extremely contaminated substance.

2.6 BUBBLE SWARM VELOCITY

A swarm of bubbles tends to rise slower than individual bubbles of the same size. As a bubble rises, liquid passes down around the sides of the bubble to fill the void continuously left behind the bubble. The net down-flux of liquid is felt by neighboring bubbles, who are themselves causing liquid down-flux. This action slows the velocity of the swarm. Marrucci (1965) used a cellular model in which the bubbles are spheres concentric within a network of spherical cells. Ignoring the wake effects of preceding bubbles, Marrucci arrived at a correction factor based on the volume fraction of gas in a bubble swarm. The velocity of a swarm of equal size bubbles is:

$$v_{\text{swarm}} = v_{\text{single}} * ((1-\epsilon)^{**2} / (1-\epsilon^{**1.67})) \dots \dots \dots (2.6)$$

where v_{single} is the velocity of a single bubble and ϵ is the gas fraction. A graph of Equation (2.6) is shown in Figure 12. The very scarce data available on bubble swarms indicate a weak decrease in velocity with increasing gas concentration. The decrease is not as strong as Equation (2.6) would indicate. This is probably due to the wake effects of preceding bubbles.

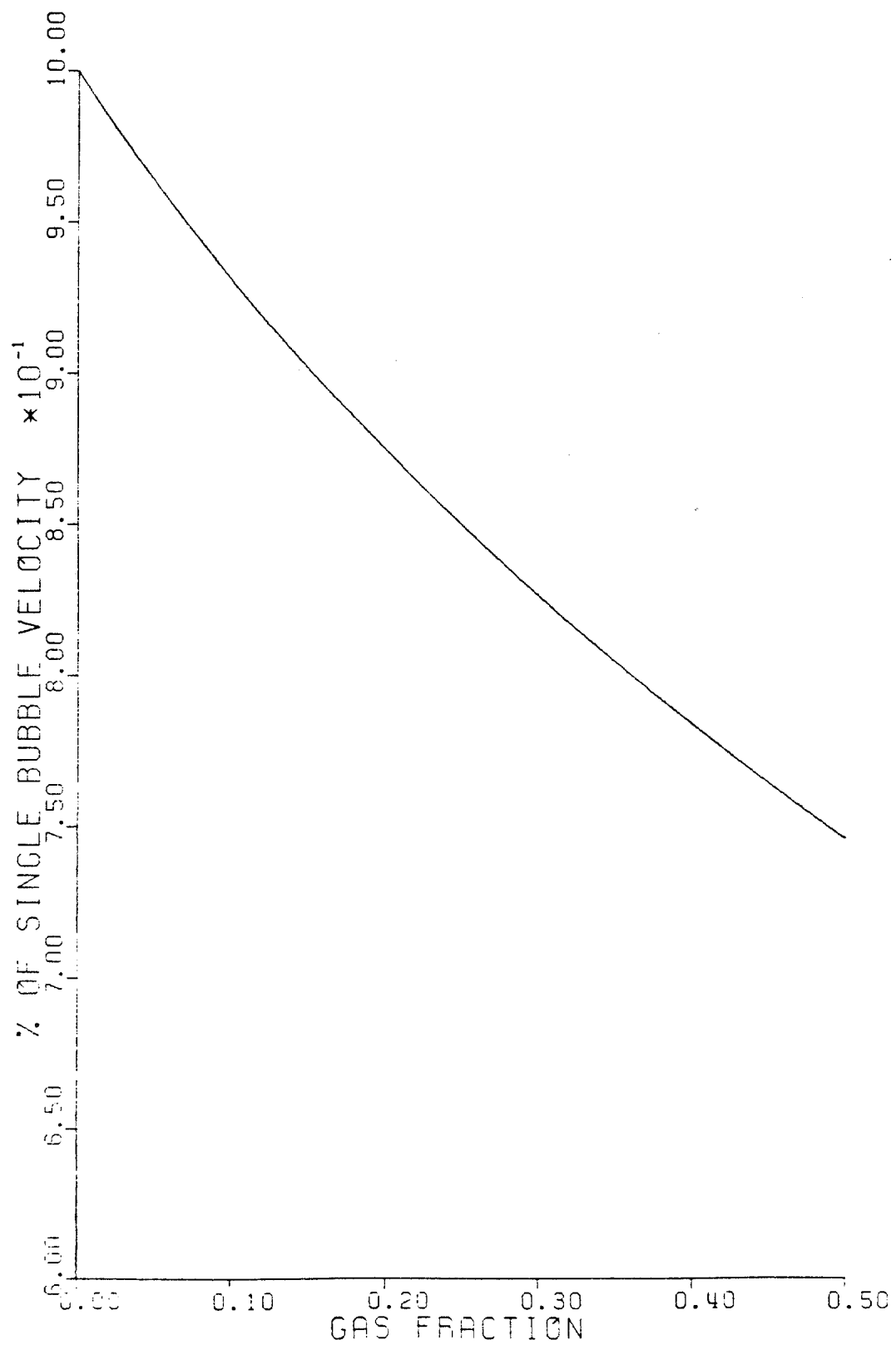


Figure 12: Ratio of swarm velocity to single bubble velocity, as a function of swarm gas fraction

2.7 ADAPTATION TO COMPUTER MODEL

A slip velocity subroutine was written for use in the computer model. As discussed earlier, the mathematics involved in modeling bubble velocities from a theoretical standpoint are both cumbersome and of questionable accuracy. The author modeled the experimental data of Peebles et al., (1953), and Haberman et al., (1954). These studies were chosen because both have extensive velocity data for a large range of bubble sizes in liquids with a wide variety of properties. Also, the experimental conditions are well recorded.

A detailed rendition of the above papers is beyond the scope of the current study. For details on the data and its analysis and interpretation, the reader is referred to the fine work of Peebles et al., (1953), and Haberman et al., (1954).

The following is a summary of the adaptation of the experimental data to the computer model. The first step was to determine equations for the terminal velocity of bubbles under laboratory conditions. Laboratory conditions imply a single bubble in an infinite, uncontaminated liquid. The equations are based on bubble size and liquid and gas properties, and are straight lines when plotted on log-log paper. Closest attention was paid to the data associated with liquids whose properties are similar to drilling fluids.

The equations, and the corresponding ranges of applicability are shown in Table 3.

The equations in Table 3 are then modified to account for wall effects (Uno et al., 1956), the presence of other bubbles (Marrucci, 1965), and fluid contamination (Ishii et al., 1980). The modifying coefficients are shown in Table 4, and the finale equations used in the computer model are shown in Table 5

No attempt is made to modify the regions of applicability for wall effects, the presence of other bubbles, or fluid contamination.

TABLE 3

Velocity equations and regions of applicability

Region number	Equation for velocity	applicability
1	$v = 276 * F_b * req^{**2} / \mu$	$Re < 2$
2	$v = 2.1 * (F_b / \mu)^{**.45} * req^{**.92}$	$req < .17 * G1^{**(-.35)}$
3	$v = .163 * F_b^{**.35} * req^{**.112} / \mu^{**.2}$	$req < G2$
4	$v = .316 * req^{**.5}$	$req > G2$
$G1 = 8.0 * 10^{**-5} * \mu^{**4} / (F_b * \sigma^{**3})$		$G2 = \sigma / (87.6 * F_b / 8.33)$

TABLE 4
Modifying coefficients

Region number	Modifying coefficients		
	swarm	wall	contamination
1	1.06	0.0	$41.3 \cdot \text{req}^{.77}$
2	1.03	0.0	$3.09 \cdot \text{req}^{.336}$
3	1.01	1.01	1.24
4	0.0	$1.17 \cdot \mu^{.045} \cdot \text{req}^{.21}$	1.1

TABLE 5
Equations used in computer model

Region number	Velocity equation
1	$v = 6.68 \cdot Fb \cdot \text{req}^{1.23} / \mu$
2	$v = .68 \cdot (Fb / \mu)^{.45} \cdot \text{req}^{.584}$
3	$v = .13 \cdot Fb^{.35} \cdot \text{req}^{.112} / \mu^{.2}$
4	$v = .27 \cdot \text{req}^{.29} / \mu^{.045}$

Chapter III
VERTICAL GAS DISTRIBUTION

3.1 BUBBLE SIZE DISTRIBUTION

As shown in the introduction, a gas kick exists as a large number of discreet bubbles. Knowledge of the specific sizes of the various bubbles is extremely important. In a shut-in well, the bubble size distribution controls the vertical distribution of gas in the wellbore over time. This is a result of bubble slip velocity being a strong function of bubble size.

The bubble size distribution is felt to be very important in a pumping well also. The vertical distribution of gas contributes significantly to the overall pressure behavior of a pumping well. Soruor (1982) conducted research indicating that two phase flow regime transitions* are strongly affected by bubble size distribution. This in turn influences the two phase pressure drop.

* Two phase flow of gas and liquid is divided into various regimes based on the behavior and appearance of the flow. Going from low gas concentration to high gas concentration, the regimes usually recognized include bubble flow, slug flow, churn flow, and annular or mist flow. For a complete description of flow regimes, the reader is referred to Taitel et al., (1980).

The initial bubble size distribution of a gas kick is primarily determined by the conditions existing when and where the kick enters the wellbore. After the kick is completely in the wellbore, bubble instability and bubble re-conglomeration control the size distribution.

It is known from experimental runs at the LSU research and training well that a wide distribution of bubble sizes exists (Mathews, 1980). When a gas kick is pumped into the well while shut-in, the first gas appears at the surface after about 5 hours, indicating moderately large bubbles. About 22 hours is required for the surface pressure to completely stabilize, meaning that small bubbles are still migrating upward until this time.

3.2 ENTRANCE CONDITIONS

The apparatus at the bottom of the LSU well through which the nitrogen is pumped is a 1.0-in. pipe with thirty-nine 0.25-in. holes drilled into the sides and a plug at the bottom. A detail drawing of this apparatus is shown in Chapter 5.

Although it would have been more realistic to place a large piece of sandstone here for the gas to pass through on the way into the the well bore, this was impractical.

At very low gas inflow rates the pipe assembly is thought to produce streams of bubbles about 0.3-in. in diameter. Tests run with 0.25-in. I.D. tubing produced bubbles of about this size in water. Up to a certain point, increased flow merely decreases the spacing between the bubbles. At low flows, the size at which a bubble will break away from a small opening is largely independent of flow rate. Surface tension is the controlling factor because the bubble must "break" a gas-liquid interface to separate itself from the hole. Sandstone will release bubbles smaller than 0.3-in. diameter, because of the smaller openings facing the wellbore. Surface tension and matrix geometry will control the size.

Although the author has no direct experimental evidence, it is felt that the bottom hole injection assembly in the LSU training well will produce a bubble size distribution similar to that produced by a sandstone reservoir at the moderate to high gas injection rates associated with a gas kick. The gas must be transported away at the same rate at which it is injected. The transport rate in the wellbore is a function of the gas concentration and the bubble size distribution. Transport rate increases with average bubble size, because larger bubbles have a higher slip velocity. It is believed that the bubble size distribution is mostly a function of gas injection rate, borehole geometry, and all the properties that affect bubble slip velocity. The chaot-

ic nature of high gas flow through a 0.25-in. tube into water seems to produce a wide variety of bubble sizes.

The current study concerns the feasibility of computing the change in the vertical gas distribution over time as a means of predicting the pressure behavior of a shut-in well. Because the LSU research and training well is used to evaluate the computer program, the author must model the bubble size distribution produced in this well.

3.3 BUBBLE STABILITY

The mechanics surrounding bubble stability are extremely complex. The cohesive forces of surface tension keep a bubble together. Inertial forces and turbulence act to break a bubble apart. Inertial forces and turbulence grow with increasing bubble size, while surface tension forces do not. Therefore, bubbles become less stable as they grow larger.

A few authors have commented on bubble stability, simply stating that above a certain size, bubbles seem to become unstable and break up. Only one reference could be found that offered explanations or equations concerning bubble stability. (Levich, V.L., 1962; pp. 395-396). Levich is a Russian physicist whose hydrodynamics book is translated into English. He refers to a number of other interesting studies, but none of these are translated.

At first Levich reasoned that if the dynamic pressure exerted by the liquid, $\rho_l U^2/2$ exceeds the capillary pressure, σ/r_{eq} , the bubble becomes unstable and breaks up. Inserting typical values for water yields a critical r_{eq} of .0031-in. This is clearly not the case.

After this, Levich thought that perhaps the dynamic pressure set up by the gas within the bubble is responsible for bubble breakup. The pressure is directed outward from inside the bubble. The liquid density and velocity in the expression $\rho_l U^2/2$ above are replaced by the corresponding values for gas. Equating these two expressions and solving for the equivalent radius yields:

$$r_{eq} = ((3\sigma)/(C_d v^2 (\rho_g \rho_l^2)^{.3333}))^{.3333} \dots (3.1)$$

Substituting what Levich suggests as typical values for filtered water yields a critical radius of 1.8 cm. Although this value is right in line with the results of the current author for swimming pool water, it may be a coincidence. It is the current author's feeling that liquid-induced inertial forces cause bubble breakup. Also, this equation does not seem valid for more viscous fluids. Viscosity does not appear in Equation (3.1). It is known from experiments with honey and water, and from experiments at the LSU research and training well (Mathews, 1980), that viscosity plays an important role in bubble stability. Viscosity lowers the Reynolds number, and therefore lessens the turbulence imp-

inging on the bubble. Viscosity has other effects which will be commented upon later.

Haberman et al., (1954) does not comment upon bubble stability directly. However, the largest equivalent radii bubbles they report using are 1.2 cm for tap water, and 3.2 cm for filtered water. This demonstrates the importance of surface tension in bubble stability. Filtered water has a surface tension of about 73 dynes/cm. The contaminants in tap water reduce this value to about 40 dynes/cm.

To study bubble stability and bubble reglomeration first hand, the author conducted experiments in a swimming pool. Bubbles were released from shot glasses and bowls. Bubbles were closely observed through a diving mask. It was found that bubble stability is very much a probability related phenomenon. In other words, a bubble increasing in size due to loss of hydrostatic pressure as it rises does not, upon reaching a certain critical size, necessarily become unstable and break up. There is a certain probability that the bubble will break up. This probability increases with bubble size and the amount of time the bubble exists.

All bubbles were released from the bottom of a pool with a depth of 9 feet. All reqs quoted were measured at the surface. A bubble's volume will increase 27%, going from 9 to 0 ft of hydrostatic head.

ity decreases the average number of product bubbles produced during bubble breakup. In doing so, viscosity shifts the average product bubble size upward.

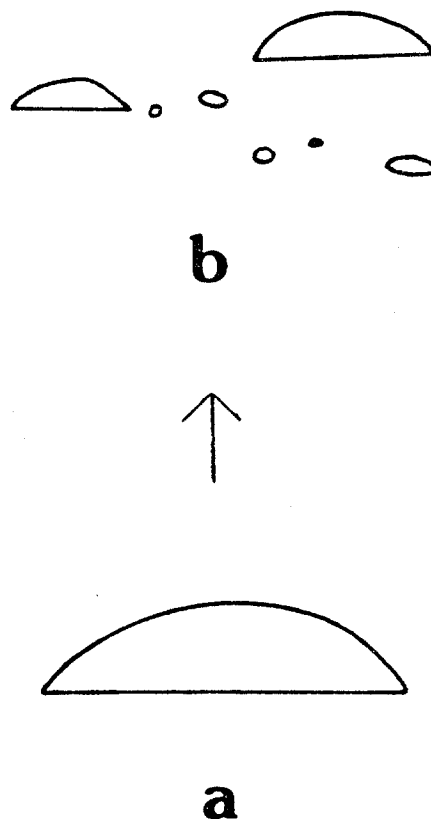


Figure 13: Typical number and sizes of product bubbles produced during bubble breakup

The mechanism of bubble breakup is as follows: for no readily apparent reason, one side of the bubble seems to get pulled to one side and downward, as shown in Figure 14. Bubble motion is slowed noticeably when this happens. The process often starts and proceeds as far as Figure 14 b, then reverts back to a normal spherical cap bubble. Other times the process proceeds all the way to bubble breakup.

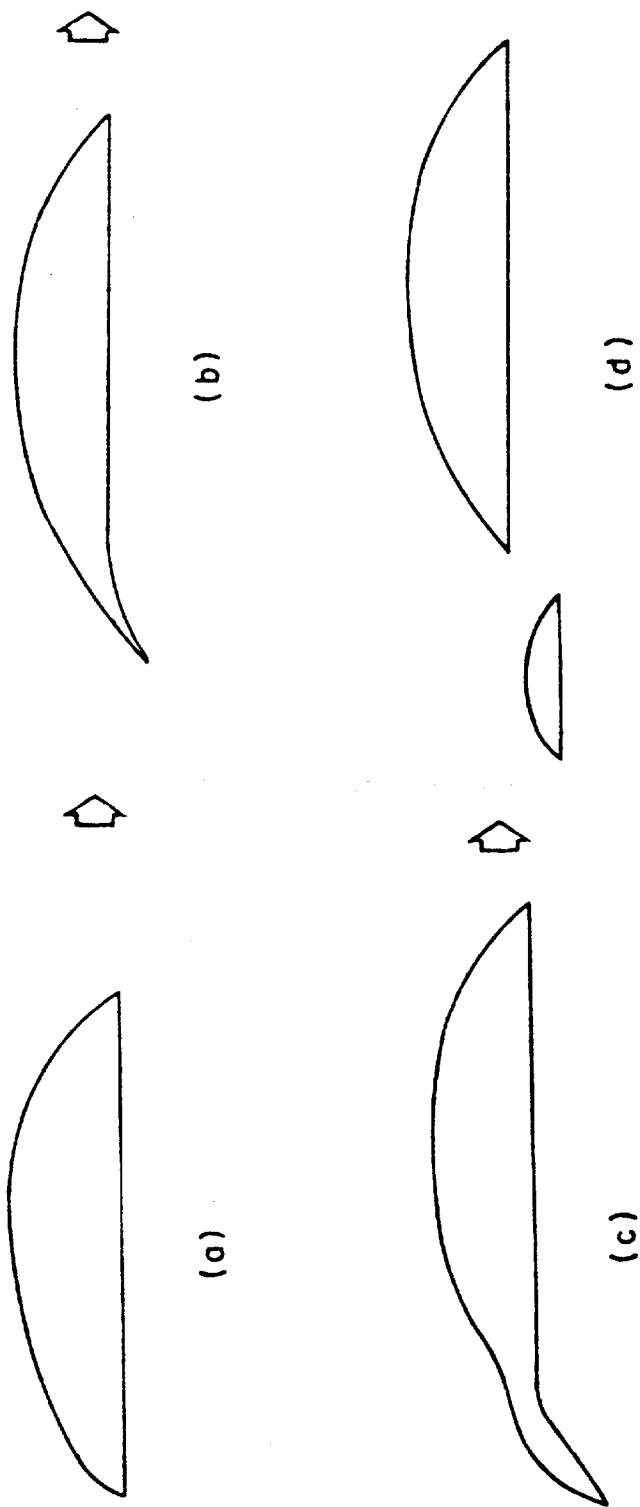


Figure 14: One form of bubble breakup

3.4 RECONGLOMERATION

Reconglomeration of bubbles happens under certain conditions. Spherical and oblate spheroid bubbles were never observed to combine with other spherical or oblate spheroid bubbles, even if they bumped one another. If directly in the path of a spherical cap bubble, a spherical or oblate spheroid bubble will combine with the spherical cap bubble about half of the time, in a manner as follows: the smaller bubble rises more slowly, and is swept to one side as the larger bubble overtakes it. The smaller bubble meanders into the wake region that travels behind the larger bubble, then moves quickly up through this wake region into the back end of the bubble. This process is shown in Figure 15. If recombination does not take place, it is because the smaller bubble never moved into the wake of the larger bubble.

If a large spherical cap bubble overtakes a smaller spherical cap bubble, often only part of the smaller bubble is drawn into the wake. This part breaks away and travels up into the back of the larger bubble, as shown in Figure 16.

It is also noteworthy that some, or occasionally, all of the product bubbles produced by bubble breakup can recombine. Typically, bubble break-up produces 4 to 12 bubbles, some reconglomeration takes place, and the result is a net increase in the number of bubbles.

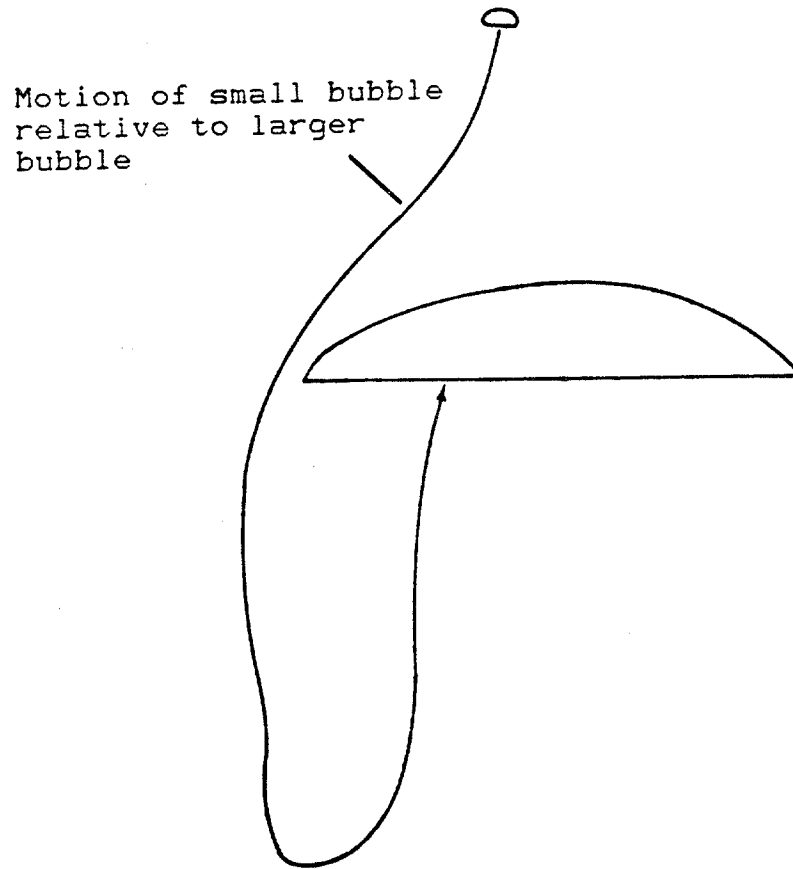


Figure 15: Mechanism by which a small bubble combines with a spherical cap bubble

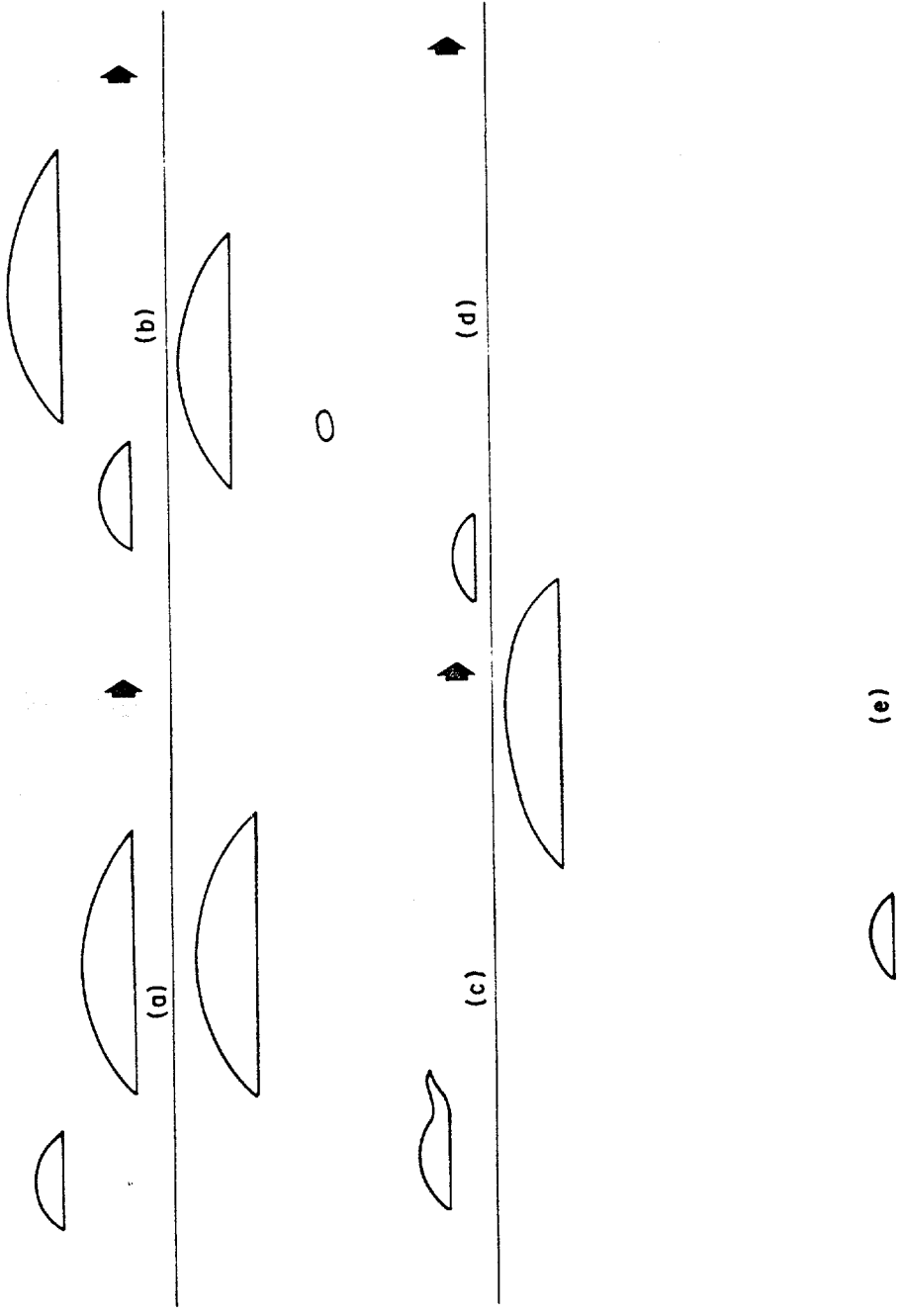


Figure 16: Typical exchange of gas between spherical cap bubbles

The author believes that much bubble break-up and reconglomeration will occur in a well that has just taken a gas kick. The gas will immediately start seeking stable bubble sizes, causing bubble breakup. Also, a lot of initial reconglomeration will take place. Large bubbles produced low in the kick zone will pass smaller bubbles produced higher up, plus the products of previous bubble breakups. Eventually, a fairly stable bubble size distribution will be obtained.

Chapter IV

DEVELOPMENT OF COMPUTER MODEL

The key factors contributing to the pressure behavior of a shut-in well that has taken a gas kick have been discussed in the preceding chapters. Before describing the computer program it is best to review the physical situation being modeled in the LSU research and training well.

Soon after the simulated gas kick enters the bottom of the well, the influences of bubble instability and bubble reglomeration create a fairly stable bubble size distribution, with a wide range of bubble sizes. The size distribution is very important because for any given mud, it and the size of the kick control the change in the vertical distribution of gas with time. This in turn determines the pressure behavior.

For a given bubble size distribution, a method had to be devised to simulate the vertical position of all the gas bubbles at any point in time. Tracking individual bubbles is of course impossible. If one were to assume an average bubble diameter of 0.25-in, there would be over one million bubbles associated with a ten barrel kick.

The gas is split up into groups, the number of which is large enough for sufficient precision, but small enough for the computer to manage. The gas is split up into groups in two ways; by bubble size, and further by intervals. The computer program uses 34 different bubble sizes to approximate the continuum of sizes that exists in a gas kick. The gas is divided into 34 groups in this way. These 34 groups are further subdivided into intervals, the number of which can be chosen each time the program is run.

Each bubble size-interval combination is referred to as a compartment. An example with 4 intervals and 3 bubble sizes, and thus 12 compartments, is shown in Figure 17. Except under one specific circumstance to be described later, a compartment retains its identity, (number of bubbles and mass of nitrogen remains constant), until it hits the gas-liquid interface at the top of the well. If it happens to be the lead compartment, it will hit the wellhead and create a gas-liquid interface for the next compartment to hit. For the purposes of calculation, all the gas represented by a compartment is first situated at the depth initially assigned to that compartment. This point then moves upward at the velocity of a bubble the size of which is represented by that compartment.

The program requires the computer to do a great number of calculations. This is due to the complexity of modeling a

gas kick, plus the fact that 10-12 hours of real time must be simulated. Cost and availability of computer time are limiting factors. These are the reasons for having an optional number of intervals. While initially evaluating new additions to the program, or exploring the effects of various conditions in the well, a low number of intervals can be chosen. When additional precision is desired, more intervals can be used.

The program lets 100 seconds of real time elapse each time it runs through the calculations. For each time through, and for each compartment, the program must look at the depth of every other compartment in order to calculate the change in hydrostatic pressure, and thus the change in size of the bubbles associated with that compartment. Because of this, the amount of computer time used in certain parts of the program goes up by the square of the number of intervals. Above 12 intervals, the cost of computer time becomes prohibitive. However, 12 intervals provides a satisfactory amount of precision.

An average bubble size distribution for use in the computer program is estimated taking account gas entrance conditions, mud properties, and stability and reglomeration criteria. This bubble size distribution is further refined by comparing the computer predicted pressure behavior with the actual pressure behavior of the LSU research and training well as a gas kick migrates upward.

For the conventional assumption of an incompressible mud, inflexible casing, and a continuous gas slug rising in a shut-in well, gas pressure is affected only by minor variations in gas temperature, and remains almost constant. Similarly, the average pressure of a swarm of bubbles of different sizes remains almost constant. However, the pressure of the larger, faster rising bubbles decreases with time while the pressure of the smaller, slower rising bubbles increases with time, until the smaller bubbles are the only ones rising in the well. The program written in this thesis accounts for this and in addition, allows for mud compressibility and outward casing expansion.

The program can only accept an even number of intervals. For each number of intervals, Table 6 lists the corresponding number of compartments, and the amount of CPU time used by LSU's mainframe IBM 3081 computer.

TABLE 6

Computer time requirements

Number of intervals	number of compartments	CPU time(minutes)
2	68	.73
4	136	2.48
6	204	5.33
8	272	9.28
10	340	14.33
12	408	20.48

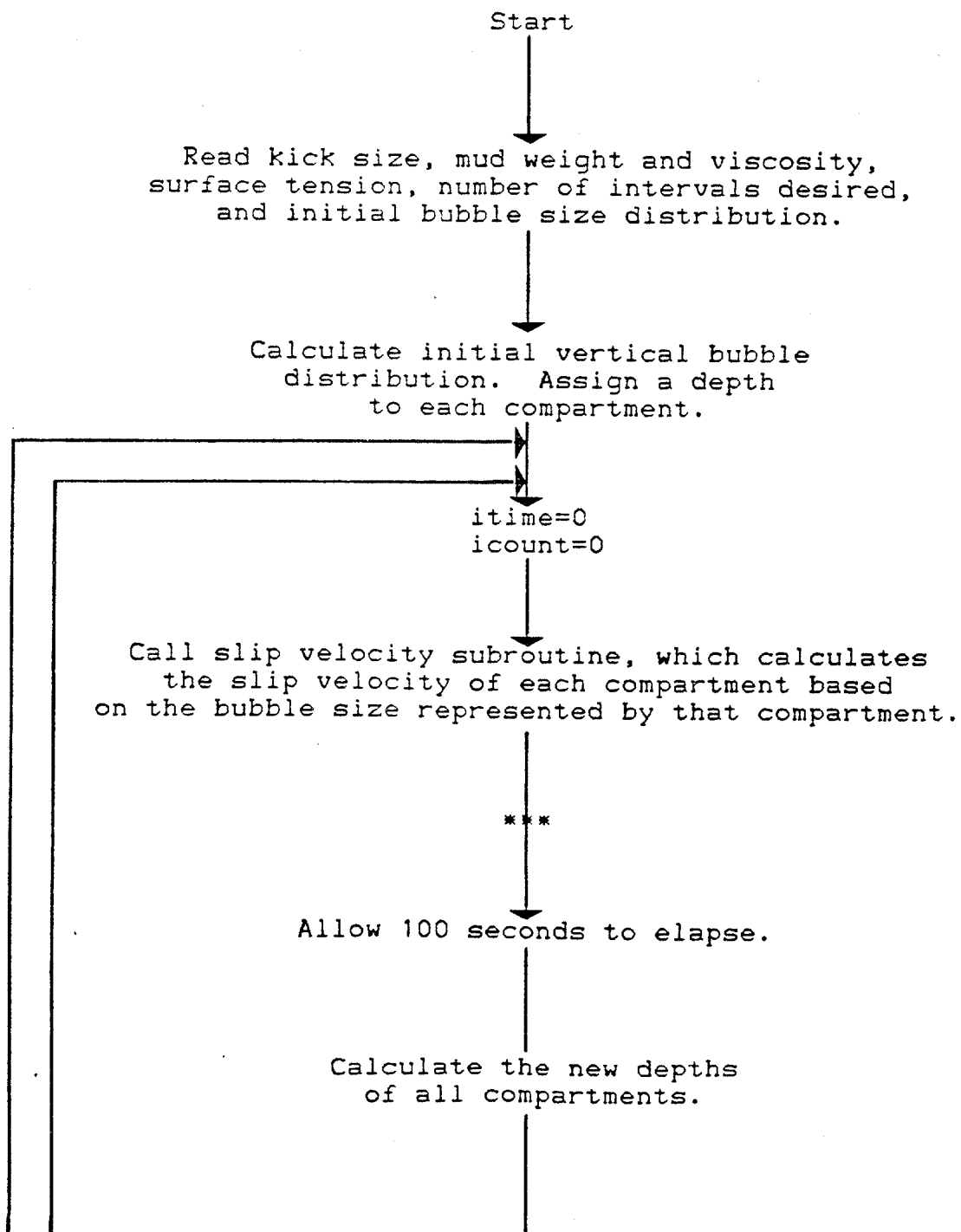
Shown in Table 7 is a flow chart illustrating the major calculations performed in the program.

The additional parts of the flow chart shown in Table 8 have been broken off for simplicity. As can be seen from the schematic diagram of the LSU research and training well in Chapter 5, there is a 7.625-in. x 2.675-in. annulus from 6000 ft. to 3000 ft., then a 2.375-in. choke line from 3000 ft. to the surface. The author saw the possibility that the annulus could transport gas bubbles to the bottom of the choke line faster than the choke line could transport gas away. In this case a backup of solid gas would buildup in the annulus below the choke line. Till the backup reduced to zero, bubble flow up the choke line would cease to exist. Solid bullet shaped slugs of gas known as Taylor bubbles would take the place of the bubbles. The program watches for this phenomenon, and makes the appropriate changes accordingly. Program calculations predict that this particular phenomenon only happens with large gas kicks, and then only for a short time.

As mentioned earlier the program does not track individual bubbles. Individual bubbles are far too numerous. Instead the program tracks compartments of many equal size bubbles. The program does however track individual slugs. Taking slugs into account, the part of the flow chart between *** and **** as labeled in Table 7 should read as that listed in Table 8.

TABLE 7

Flow Chart: Main Program



↓

Calculate the new bubble sizes, and the total amount of gas expansion from all bubbles based on changes in temperature, Z factor, and pressure. The pressure change at this point is based on loss of hydrostatic head only.

↓

Divide the expansion by 100. This is done to save computer time. For an average size kick in the LSU well, the compressibility of the mud, and the expandibility of the casing is about 1% of the average expandibility of the gas.

↓

Calculate the surface pressure increase due to this adjusted expansion based on the combination of expandibility of the casing and compressibility of the mud.

↓

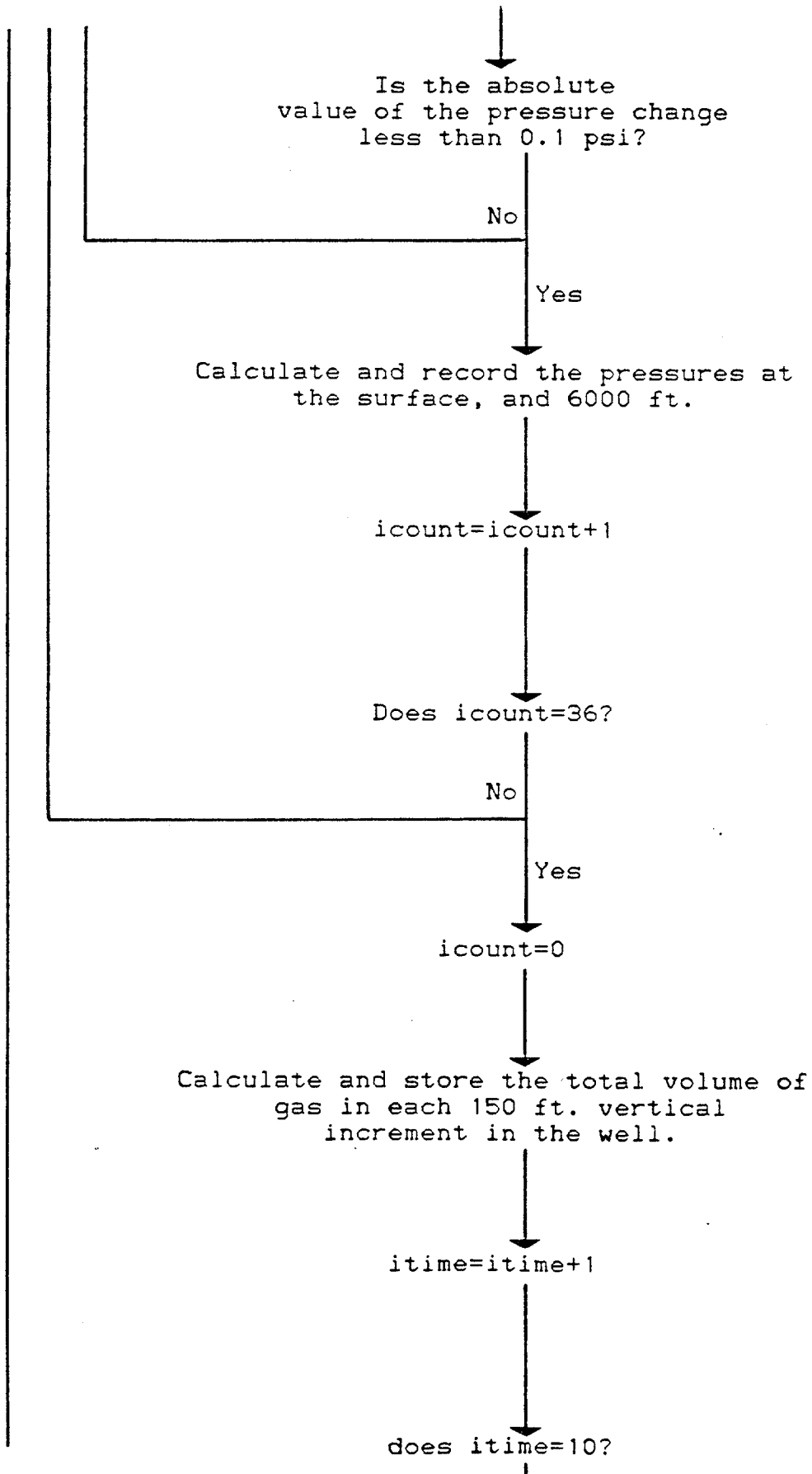
Call the PNEW subroutine, which calculates the true pressure for each compartment based on the new surface pressure, plus the pressure exerted by the gas and mud above each compartment.

↓

Calculate the new bubble sizes and the new gas expansion or contraction based on the new pressure and Z factor at each compartment.

↓

Calculate the surface pressure change; same as above.



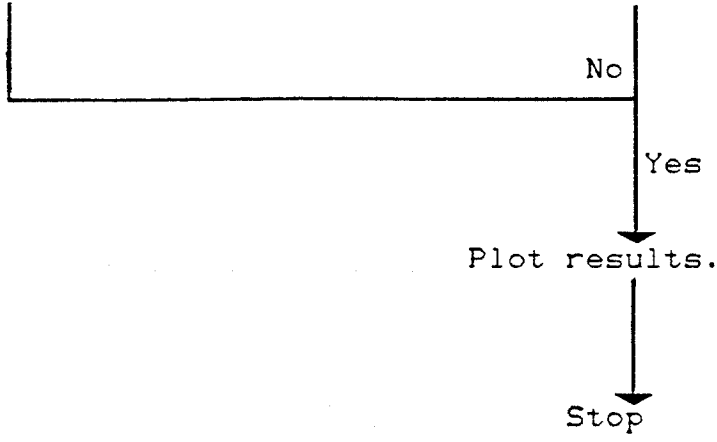
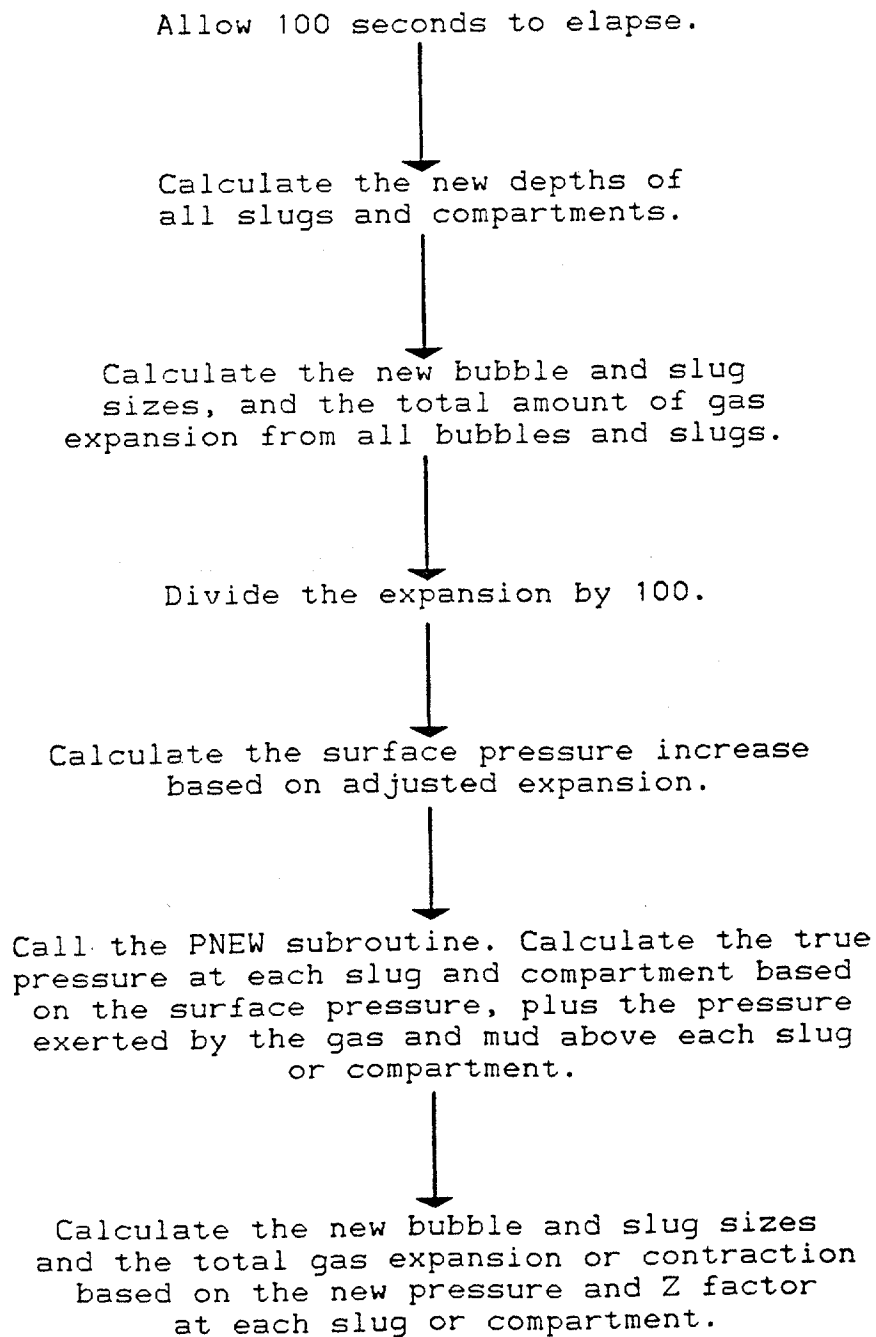


TABLE 8

Additional parts of flow chart.



4.1 LIMITATIONS OF PROGRAM

For several reasons, the program written for this thesis is not suitable for field use. The program models the geometry of the LSU research and training well. Therefore the program predicts the pressure response of that well only.

A more generalized program is needed for use in the field. Such a program would require the input of well dimensions, mud properties, pit gain, rate of pit gain, and stabilized casing and drill pipe pressures.

The concept of watching individual compartments of gas as a means of calculating the pressure response is also unsuitable for field use. The method requires far too much computer time to be practical.

Some sort of simple but clever algorithm to account for both the upward migration and spreading out of the gas is needed. Gas fraction as a function of time and depth would probably be most appropriate. It is hoped that once the behavior of a gas kick in a shut-in well is better understood, a simplified empirical model for calculating the pressure response of the well can be devised.

Chapter V

EXPERIMENTAL PROCEDURES

Actual experiments with the LSU research and training well were carried out to check and refine the performance of the computer program. LSU operates a complete blowout prevention research and training center. The facility got its start when the Goldking Production Co., after drilling a 10,000 ft. dry hole, donated the well to LSU. Completion work and surface facilities were provided by grants of equipment, services and money from 53 oil and oil service companies, and the U. S. Minerals Management Service.

The subsurface configuration of tubulars in the well was chosen so the well would exhibit the same hydraulic and pressure behavior during well control operations as a well being drilled from a floating drilling vessel in 3000 ft. of water, that has drilled through 3000 ft. of sediments. The effect of locating the BOP at the seafloor is modeled in the training well using a Baker packer and a Baker triple parallel flow tube as shown in Figure 18, which shows the subsurface configuration of the LSU research and training well. Subsea flow lines connecting the simulated BOP to the surface are modeled using 2.375-in. tubing. Drill pipe is simulated with 6000 ft. of 2.875-in. tubing. To simulate a gas

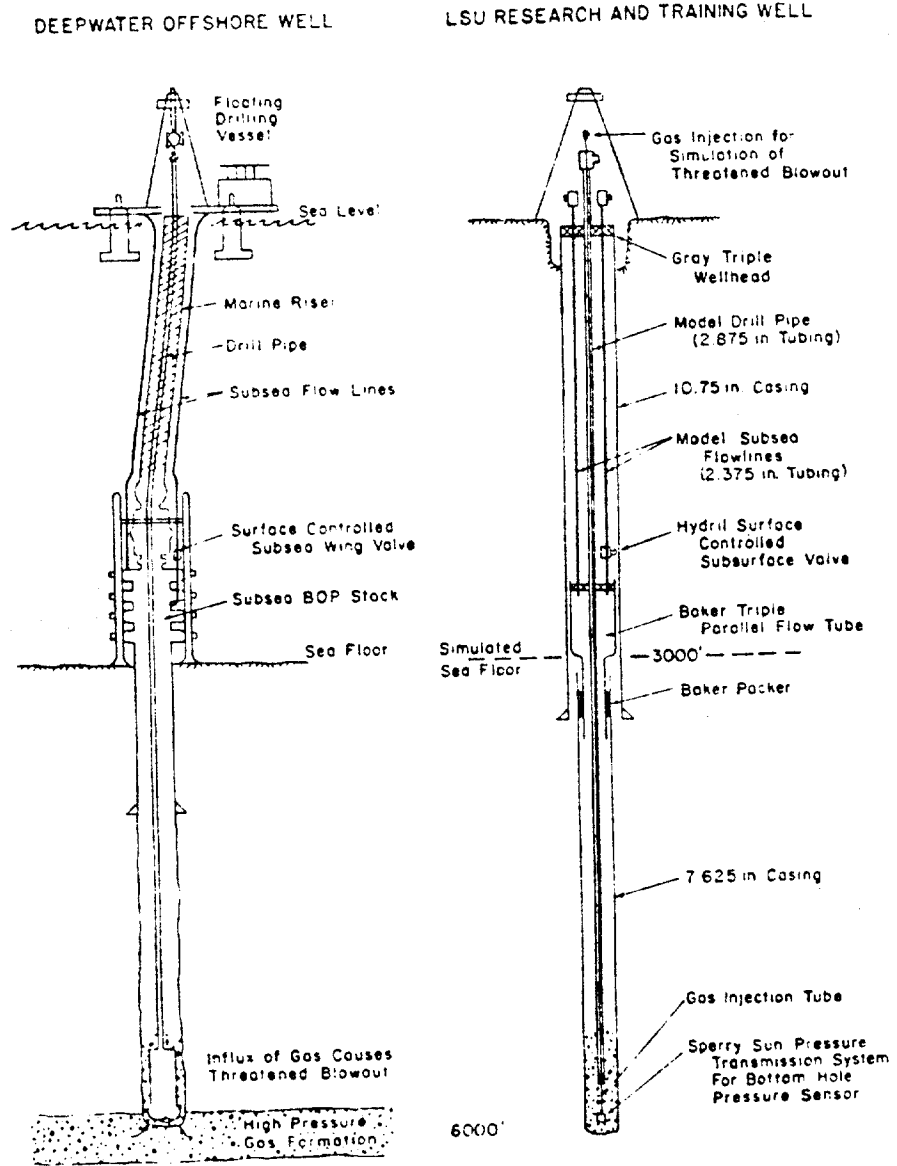


Figure 18: Subsurface configuration of the LSU research and training well

kick from a high pressure gas formation, nitrogen is injected through 1.315-in. tubing, which was placed inside the 2.875-in. tubing.

A Sperry Sun pressure transmission system was placed at the bottom of the nitrogen injection line to allow continuous surface monitoring of the bottom hole pressure during simulated well control operations. The pressure signal is transmitted through 0.125-in. O.D. capillary tubing which is strapped to the 1.135-in. tubing. A check valve located at the bottom of the nitrogen injection line allows this line to be isolated from the system after the gas kick is placed in the well. A simulated gas kick is placed in the well with a nitrogen truck. The gas enters the annulus through the bottom hole assembly shown in Figure 19.

Before the entire kick is pumped in, the well is shut-in. Continued pumping of nitrogen raises the pressure in the well, as usually happens when a real well takes a kick. The nitrogen flowing into the well is measured with a Daniel gas flow computer. This digital computer, and the related remote sensing equipment, was added to the nitrogen injection line as part of this thesis. When the desired amount of gas is in the well, the pumping is stopped. The bubbles are allowed to migrate to the surface. During this time, pressures increase at all points in the wellbore. The bottom hole pressure, and the pressure at the top of the choke line are both recorded on a strip chart. When all the bubbles

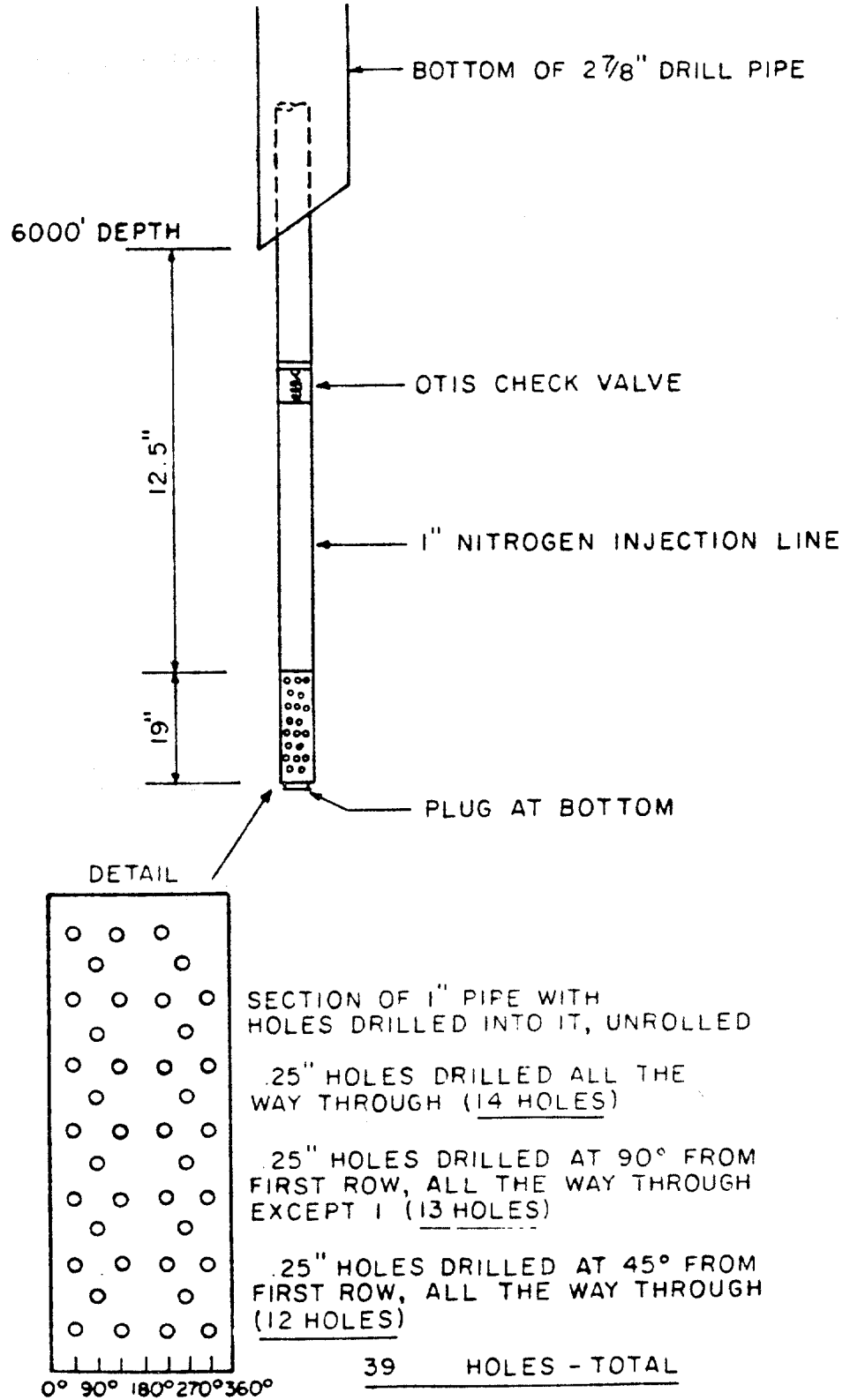


Figure 19: Nitrogen injection at the bottom of the LSU research and training well

that will migrate upward have reached the top, pressures stabilize. At this point in time, there is a solid slug of gas at the top of the choke line. Some small bubbles can be captured by the gel strength of the mud.

At this point it is desirable to completely circulate the well. Gas was vented from the top of the well through a gas flow computer. Choke pressure was reduced from 2250 psi to about 700 psi during venting. After 13.5 minutes of venting, circulation began. Pump speed and choke position were set so that choke pressure remained in the range of 400-700 psi as the well was circulated. Mud started to appear after 6.2 minutes of pumping. For the next 55 minutes a mud gas mixture circulated out of the well. After a total of 61.2 minutes of circulation, the presence of gas ceased, and only pure mud came out of the well. Mud samples were taken several times during circulation. Average mud properties are reported in Table 9. Gel strength vs time is shown in Figure 20.

TABLE 9

Average mud properties for the 1984 experiment

readings from Fann Viscometer		plastic viscosity - 12 cp
		yield point - 5 lb/100 ft**2
rpm	dial reading	mud composition:
600	29	3.5% oil
300	17	5.0% solids
200	11.5	91.5% water
100	7	

average mud sample temperature - 90° F

mud weight - 8.9 ppg

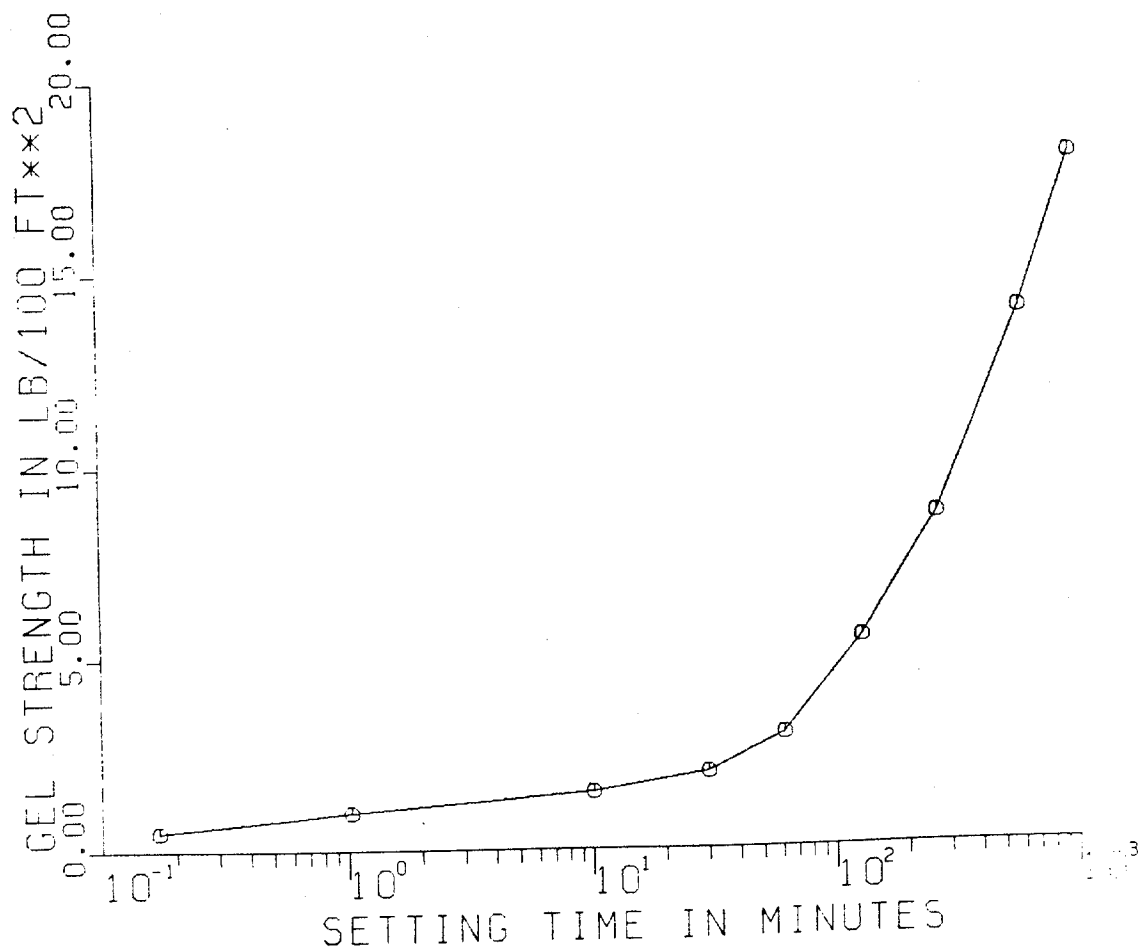


Figure 20: Gel strength vs time for the 1984 experiment

Chapter VI

RESULTS

The results of two experimental runs at the LSU research and training well were used in the preparation of this thesis. The dates of the experiments are 4/30/82 and 10/23/84. The 1982 experiment involved monitoring the surface choke line pressure and the bottom hole pressure only. The experimental and computer generated plots of pressure vs time are shown in Figure 21. The bubble size distribution in the computer program was adjusted to yield as close as possible agreement between the experimental and computer generated plots. This bubble size distribution is shown in Figure 22.

The 1984 experiment included measuring the gas pumped into the well, in addition to the pressure measurements of the 1982 experiment. Also, to enable a more detailed analysis of the results, gas flow, mud flow, and choke and bottom hole pressures were recorded as a function of time as the well was circulated. Circulation took place 25 hours after the kick was initially pumped into the well. It was found that the gel strength of the mud captured a small amount of gas at certain points in the well. The computer generated and experimental plots of pressure vs time are shown in Figure 23. The bubble size distribution used in the computer

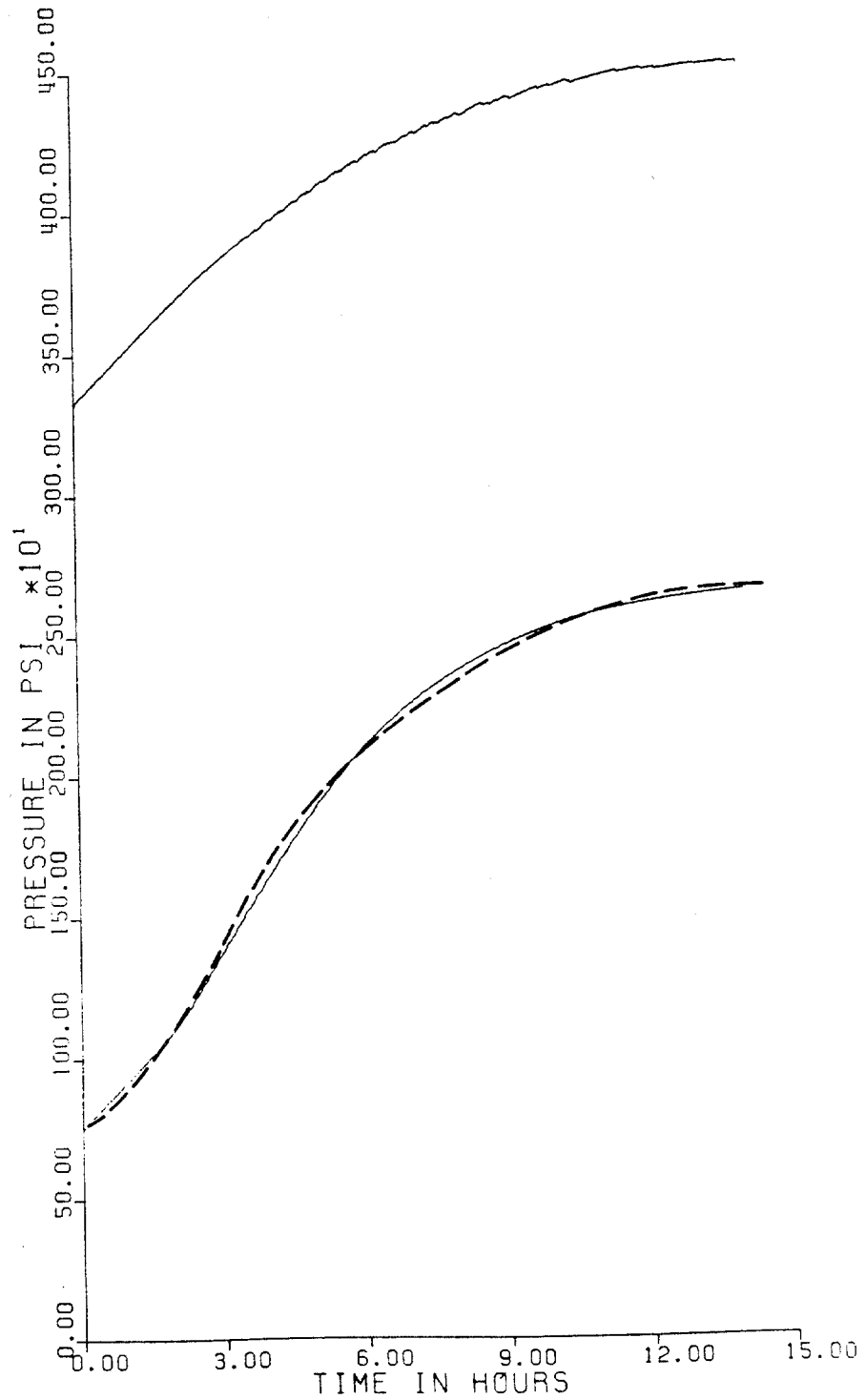


Figure 21: Pressure vs time for the 1982 experiment. Solid line is computer generated data, dotted line is experimental data

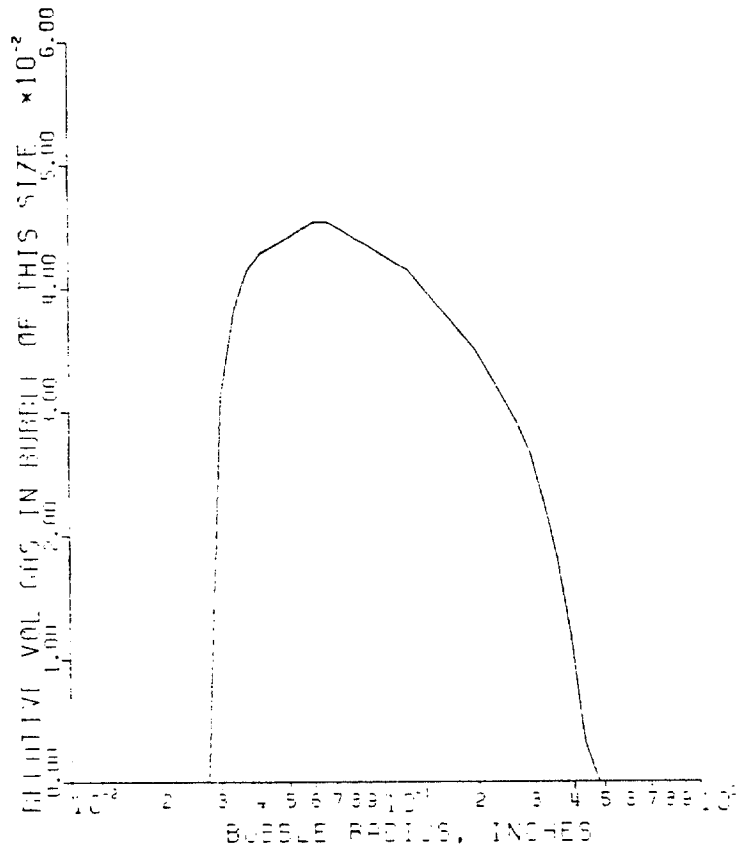


Figure 22: Approximate average bubble size distribution of the gas kick for the 1982 experiment

generated plot is shown in Figure 24. No explanation could be determined for the sharp changes in the slopes of the experimental pressure vs time plots in Figure 23. The changes occur at $t=1.12$ hours and $t=1.24$ hours.

Two interesting contrasts between the 1982 and 1984 experiments are differences in the initial rate of pressures increase, and the discrepant pressure stabilization times. The 1982 experiment has an initial pressure creep of 121 psi/hr, and a stabilization time of 14.8 hours. The 1984 experiment had an initial pressure creep of 538 psi/hr, and

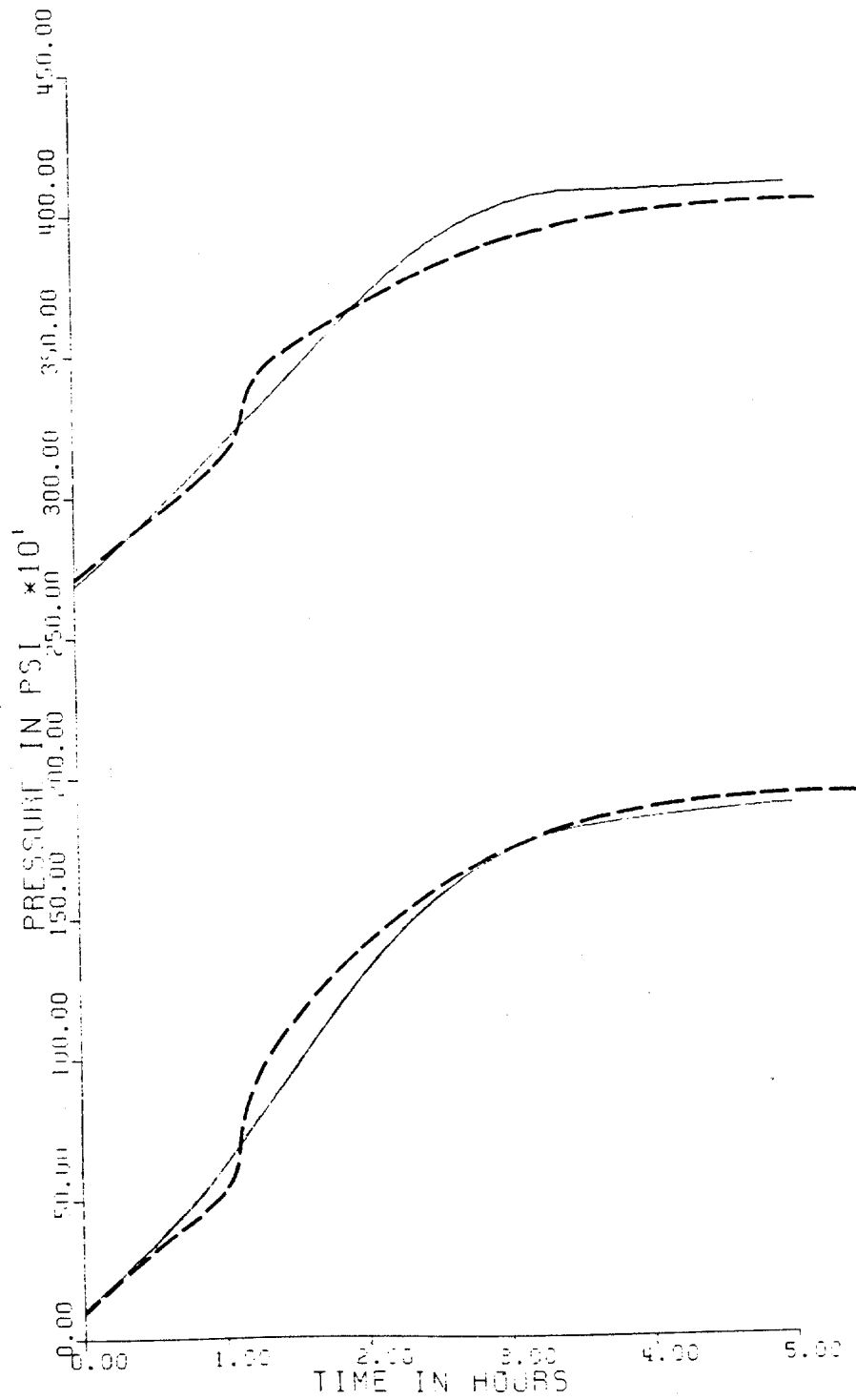


Figure 23: Pressure vs time for the 1984 experiment. Solid line is computer generated data, dotted line is experimental data

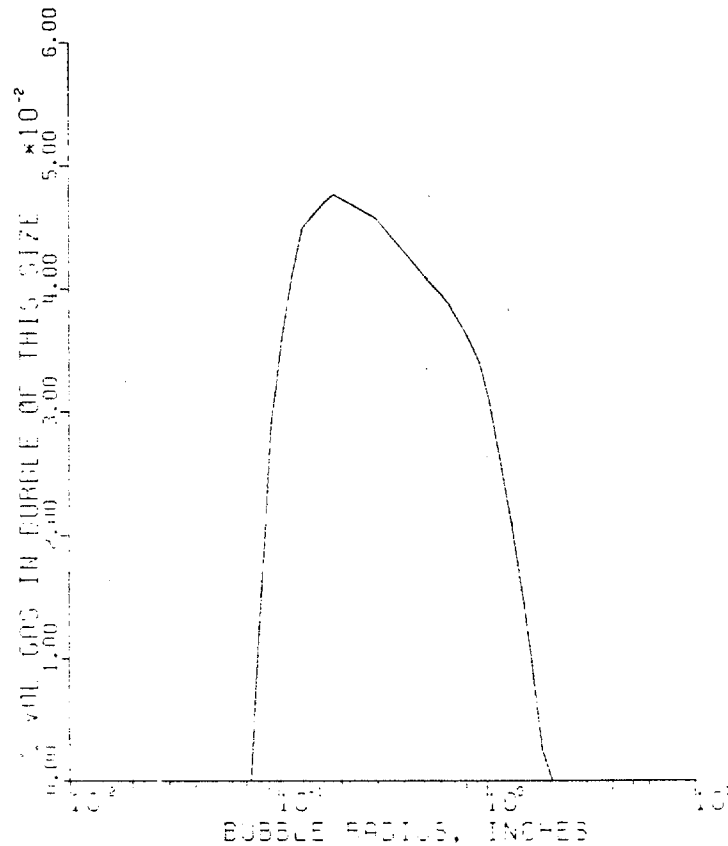


Figure 24: Approximate average bubble size distribution of the gas kick in the 1984 experiment

a stabilization time of 4.8 hours. These are rather wide variations, and exist in spite of the fact that the mud properties were approximately the same in the two experiments.

There was only one major difference between the 1982 and 1984 experiments. The kick pumped into the well for the 1984 experiment was the first one for several days. The mud was free of tiny entrained gas bubbles. Several other kicks had been pumped the same day before the kick for the 1982 experiment. This means that the mud was full of tiny entrained gas bubbles.

There are two possible explanations of why the presence of these tiny bubbles can so greatly alter the rate of upward gas migration. The real influence is probably a combination of these two effects. Firstly, the presence of the small bubbles creates a two phase viscosity which could yield a much higher apparent viscosity to a gas bubble than would be measured by a conventional viscometer. An increase in the apparent viscosity would slow upward bubble movement. Secondly, the occurrence of the small bubbles could adversely influence the stability of larger bubbles. Greater instability would shift the bubble size range downward. The rate of upward gas transport would be lessened because smaller bubbles travel more slowly than larger ones. In the computer program, the stability influence is assumed to be the only one acting. Thus, only the bubble size distribution is adjusted to make the computer program agree with both experimental runs. No adjustment is made for a two phase viscosity.

Shown in Figure 25 is gas and mud flow out of the well, and choke and bottom hole pressures all recorded vs time. Although pump speed was varied somewhat during circulation, for ease of interpretation, the data is modified to show a constant pump speed. There is a high initial gas flow rate because the well is being vented under high pressure. Pressure decreases due to opening of the choke. Pressure increases due to closing of the choke while the pump is run-

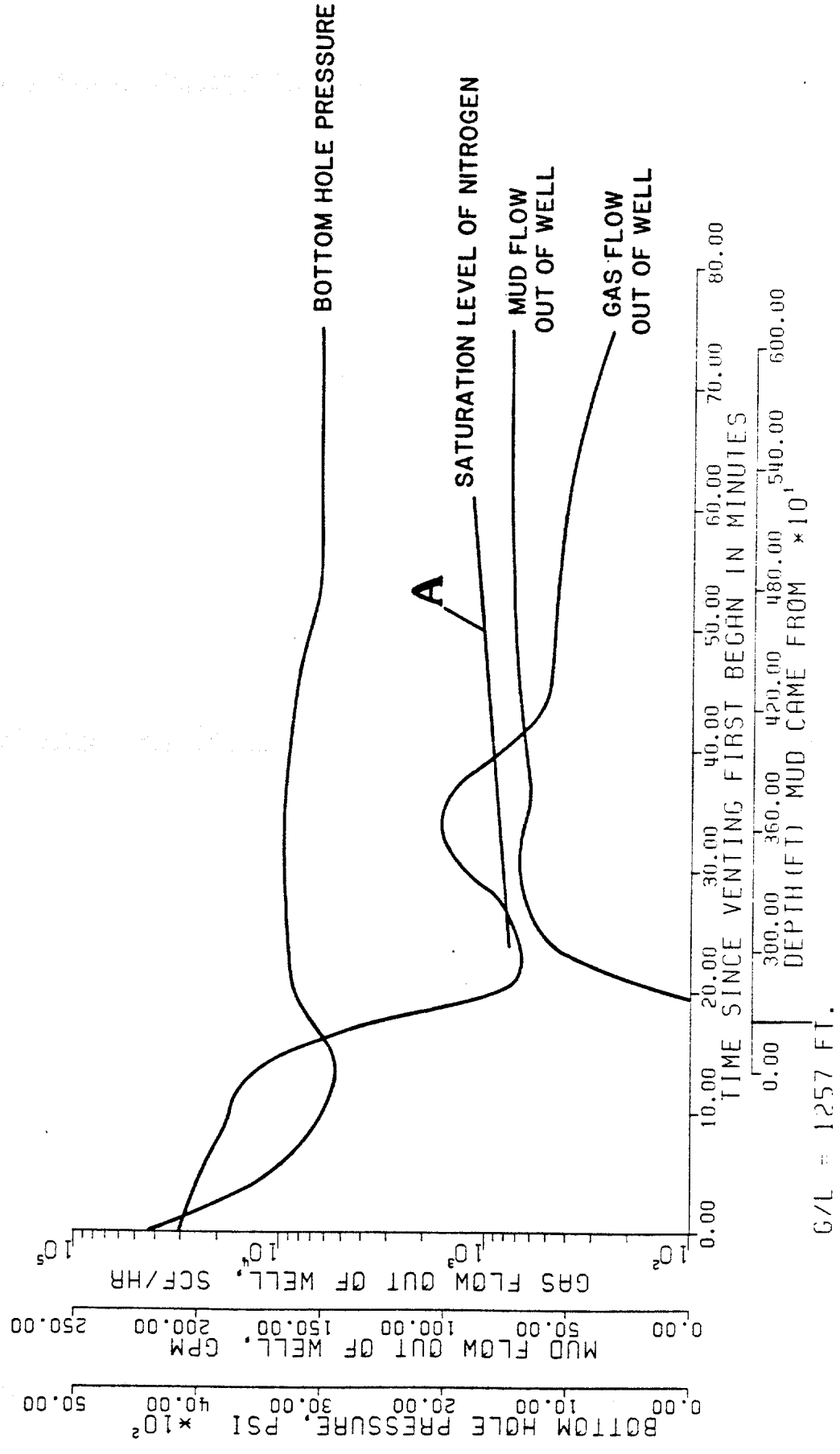


Figure 25: Gas flow(scf/min) and mud flow(gpm) out of the well, and surface choke and bottom hole pressures, all vs time

ning, or due to increase in hydrostatic head. The pump was started after 13.5 minutes of venting. Mud started to appear after 6.2 minutes of pumping. This was followed by 55 minutes of a mud gas mixture, after which only mud flowed out of the well. Also shown in Figure 25 is the saturation level of dissolved nitrogen in water corresponding to the pressure in force at each point in the well when circulation began. For example, take point A on Figure 25, corresponding to $t=50$ minutes. Mud flowing out of the well at this time started at $D=4600$ ft. when circulation began. The stabilized pressure before gas venting at this point was $p=3800$ psi. And the saturation level of dissolved nitrogen at this pressure is shown as point A.

Figure 25 also shows the depth of the mud before circulation. As can be seen, the mud in the depth range $D=3190$ ft. to $D=3970$ ft. contained more than its saturation level of dissolved nitrogen. This is felt to be small bubbles captured by the gel strength of the mud. There are no entrained gas bubbles below $D=3970$ ft. because the gel strength of the mud did not have enough time to set up before all the gas had passed by. Thus, the amount of gas captured was below the solubility saturation level. How the gel strength grows with time can be seen in Figure 20. The reason for the lack of entrained gas bubbles above $D=3190$ ft. is not completely understood, especially if the entrained bubbles came into existence when the kick was first

pumped into the well. The entrained bubbles could be the products of bubble break up, in which case there is a possible explanation. Recall that the annulus/chokeline interface is at 3000 ft. The chokeline has an I.D. of 1.995-in. It is felt that the sides of the chokeline act as confining walls and inhibit bubble break up. If this is true then there would be no source of tiny bubbles in the chokeline through bubble break up. Following these concepts, we would expect a rising gas concentration from 6000 ft. to 3000 ft., then a drop-off in the gas concentration. The unexpected drop-off from D=3600 ft. to D=3000 ft. could be due to diffusion of nitrogen from the oversaturated mud in the annulus to the undersaturated mud in the chokeline.

The program also gives a "picture history" of the gas migrating up the wellbore. The individual "pictures" are given at regular time intervals. They show the vertical gas concentration averaged out over thirty 150 ft. intervals. The history is shown in Figure 26 for the 1982 experiment, and in Figure 27 for the 1984 experiment. These figures demonstrate the spreading out of the gas contaminated region.

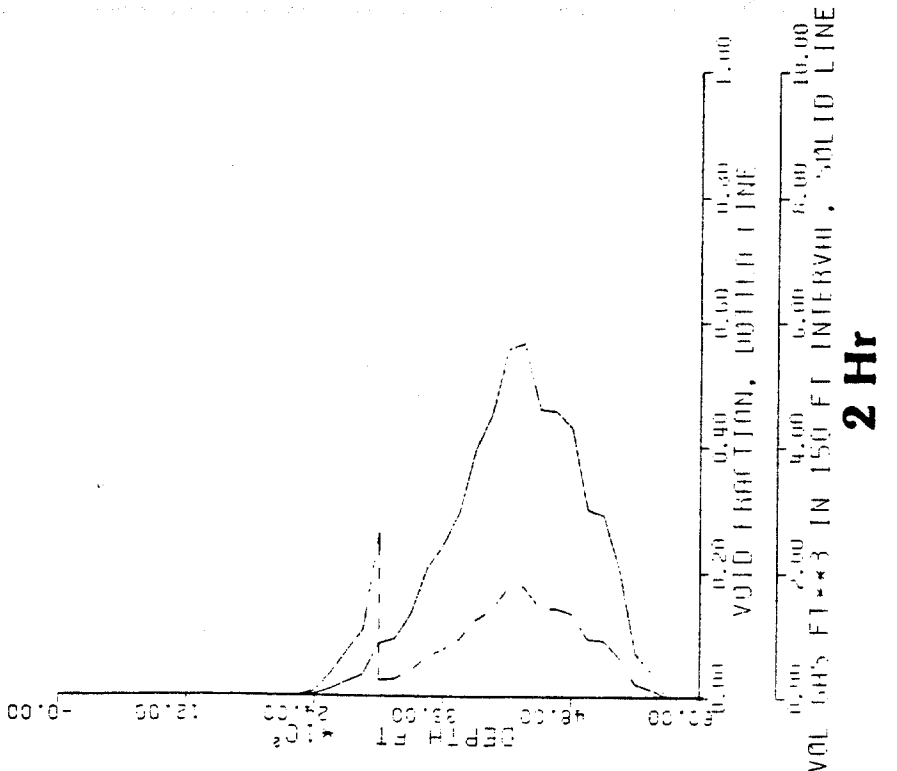
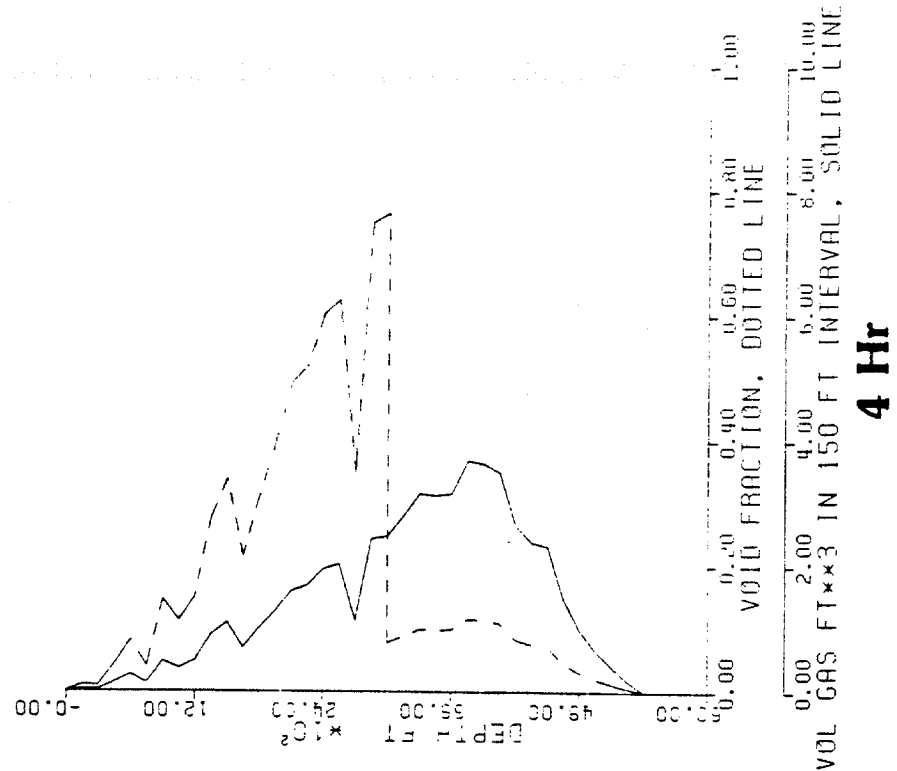


Figure 26: Computer generated picture history for the 1982 experiment

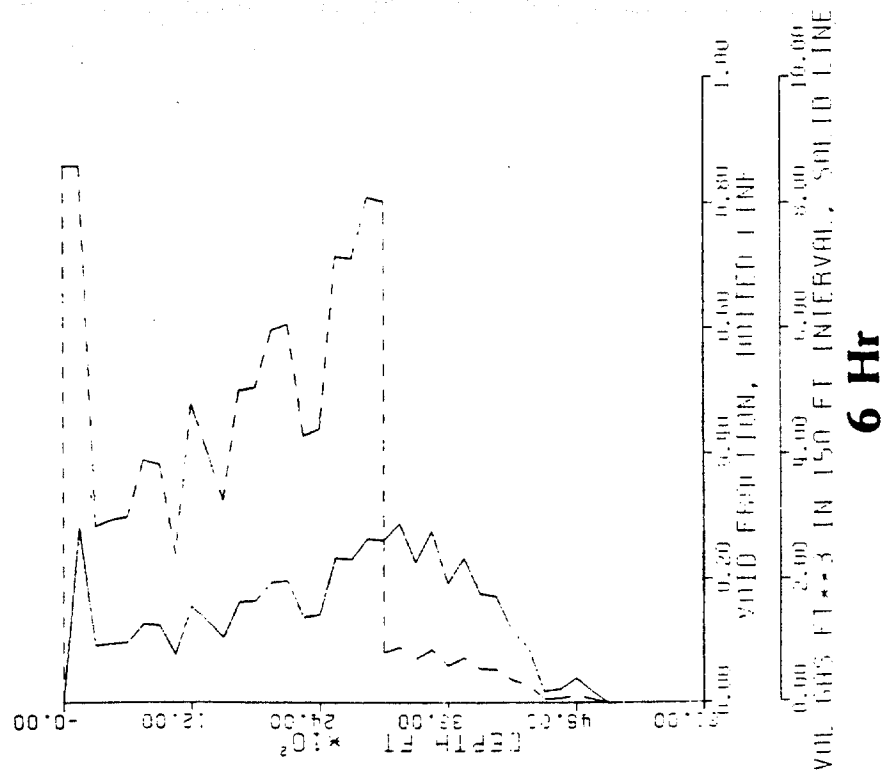
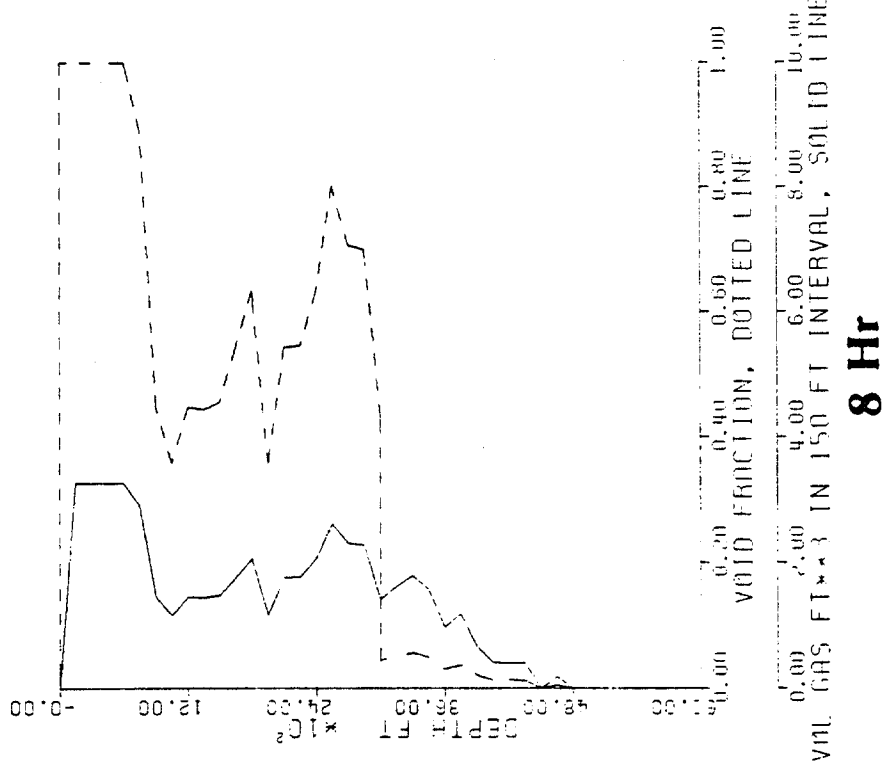


Figure 26 continued

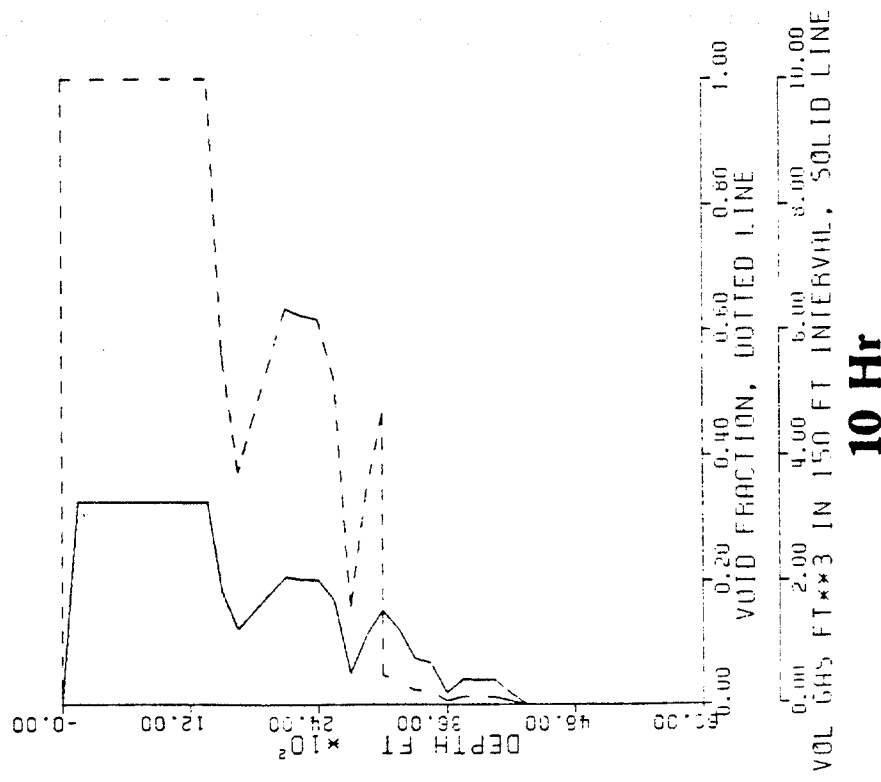
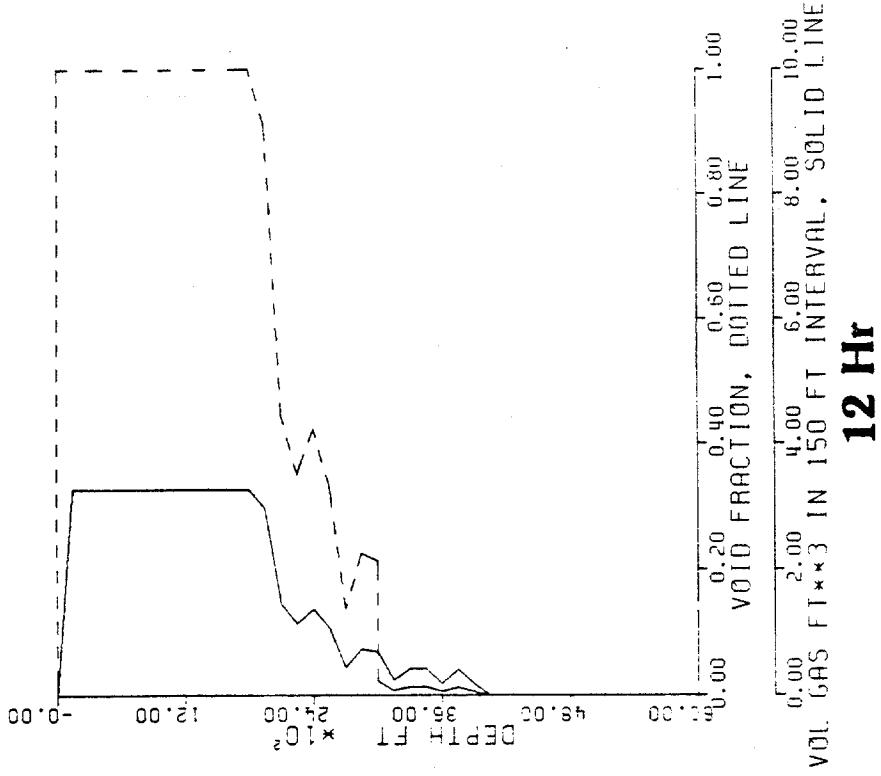


Figure 26 continued

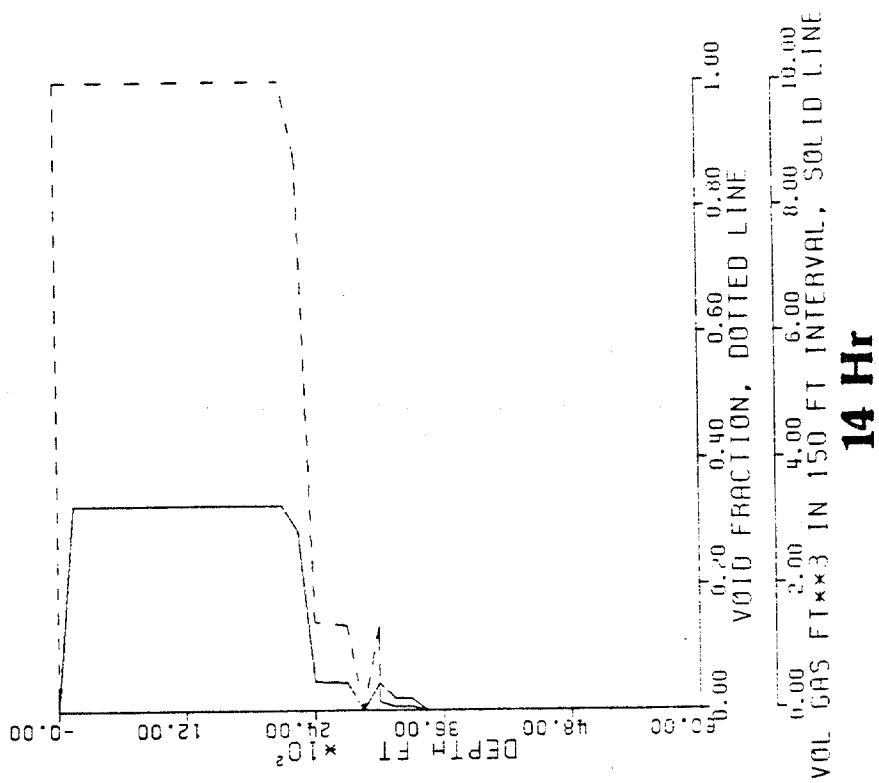


Figure 26 continued

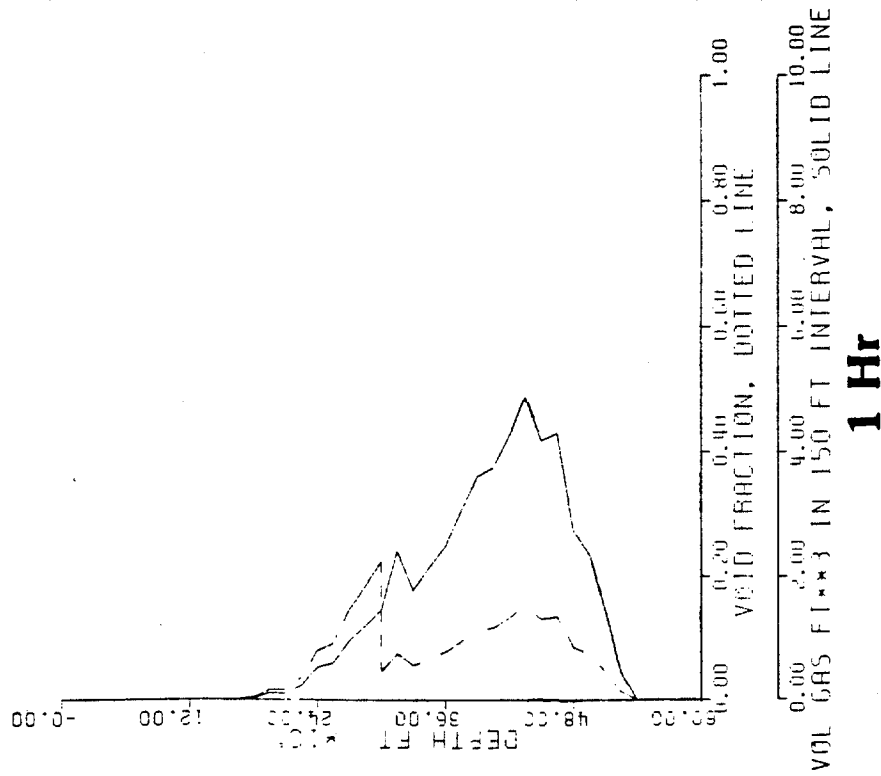
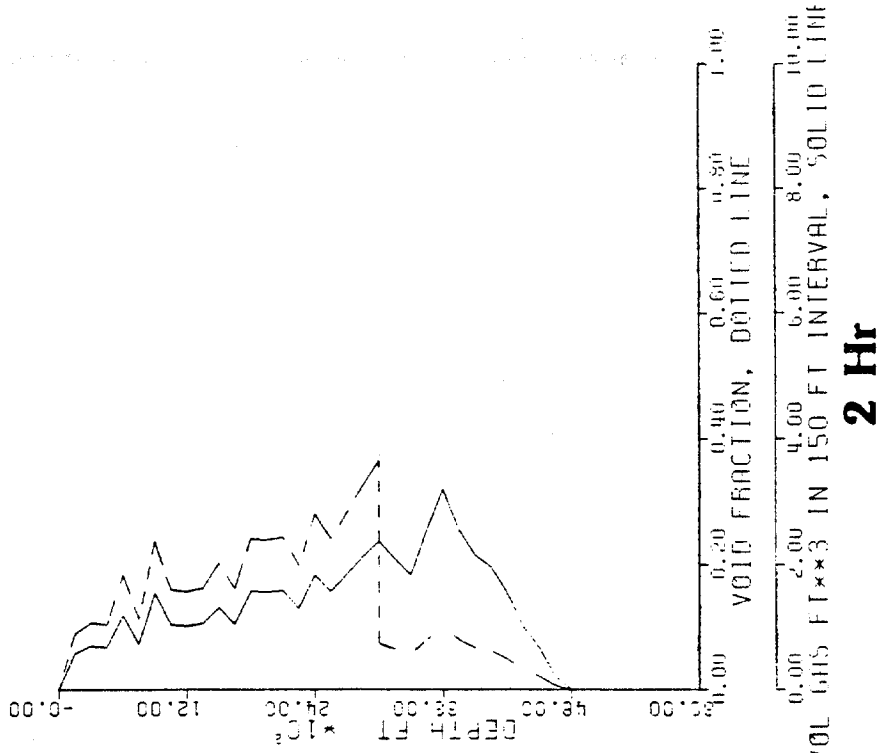


Figure 27: Computer generated picture history for the 1984 experiment

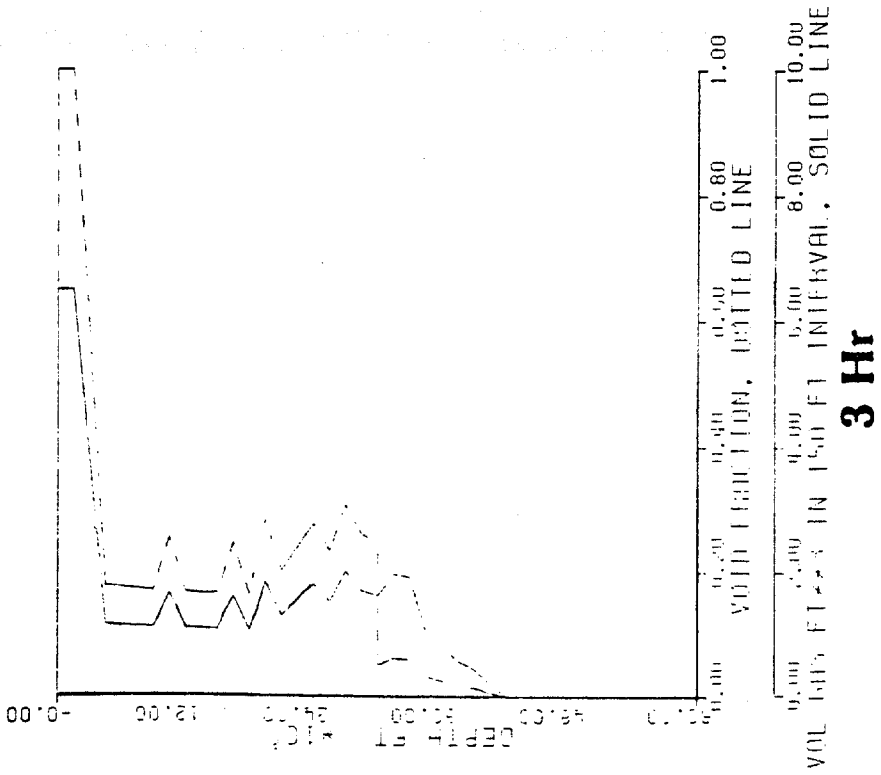
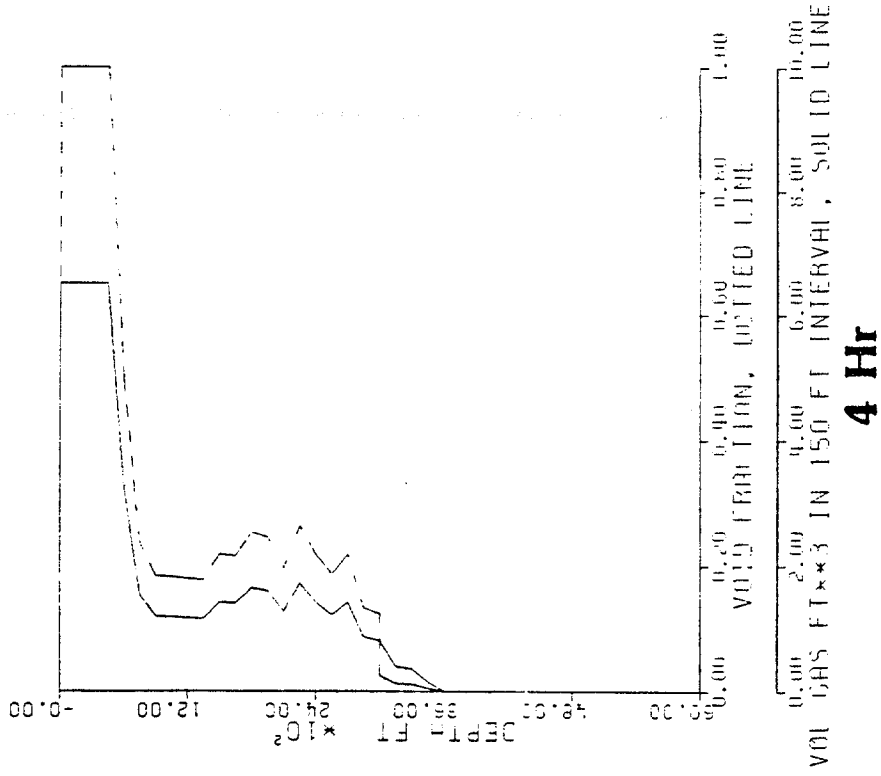
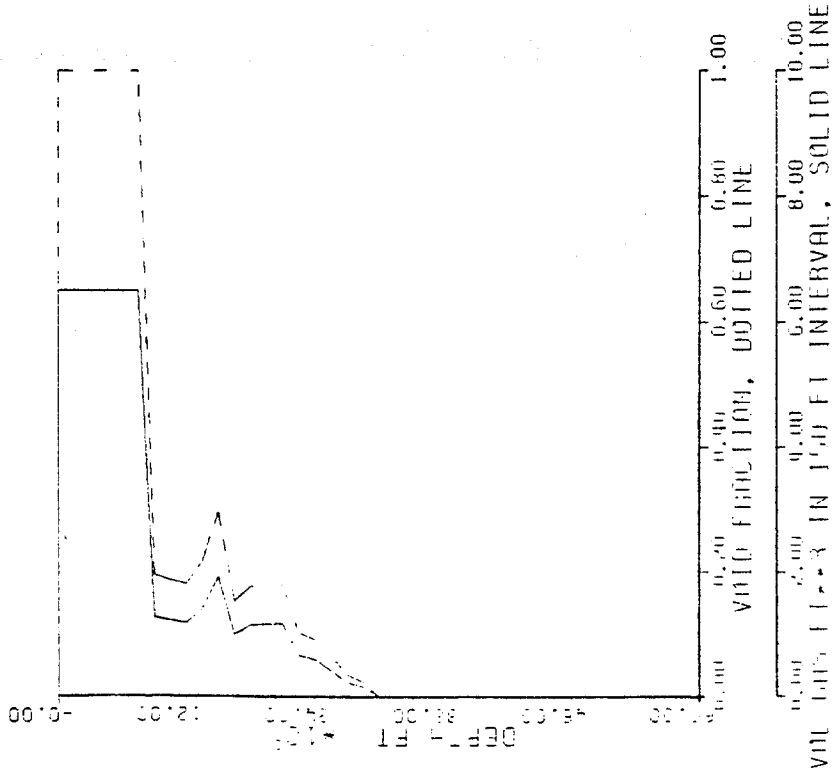
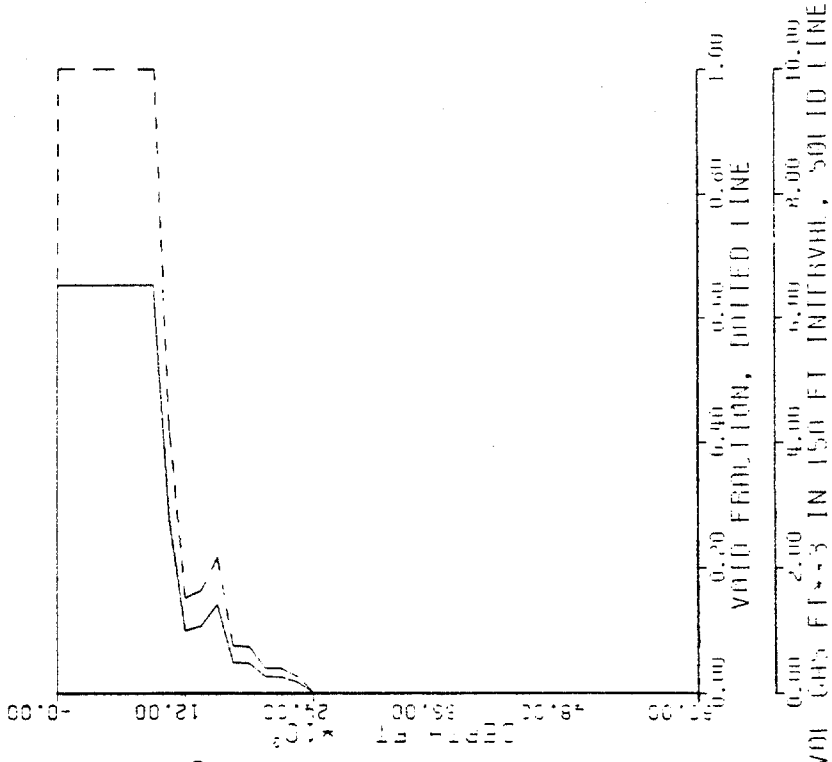


Figure 27 continued



5 Hr



6 Hr

Figure 27 continued

Chapter VII

CONCLUSIONS

As a result of the combination of computer and experimental study of gas kicks taken in a shut-in well, the following conclusions can be drawn:

1. The assumption made by earlier authors that a gas kick remains as a continuous slug during upward gas migration was shown to be invalid.
2. A computer program can be used to back out the approximate bubble size distribution of a gas kick when pressure creep data on gas migration in a shut-in well is available.
3. The computer program can give a "picture history" of the vertical distribution of gas at regular time intervals as the kick migrates upward.
4. The presence of small gas bubbles significantly lowers the rate of upward gas migration in a shut-in well.
5. It is felt that reasonably accurate modeling of the elongation and upward movement of the gas

contaminated zone can be extended to a pumping well where a gas kick is being circulated out. This would make possible better well control simulations for operators. It would also make possible more realistic well control simulators used in training field personnel.

6. A program that can predict the pressure behavior of a pumping well could be modified to compute the choke pressure profile necessary to maintain a constant bottom hole pressure.

Chapter VIII
RECOMMENDATIONS

Through the experience gained from this research, the following recommendations for further study on this topic can be made. It is believed that following these recommendations will result in better and more useful data.

1. Use of a mud with a higher gel strength, and a gel strength that sets up sooner, would yield more useful data on bubbles being captured by the mud. The low gel strength mud used in the 1984 experiment captured only enough gas for the mud to be at about saturation level. The mud could be near saturation level from the passing of larger previous bubbles. The use of a high gel strength mud will capture much more than the saturation level of gas. Inferences as to where and how much bubble break up is occurring can hopefully be made from this data.

2. The well should be circulated as soon after pressure stabilization as possible. This will prevent an undue amount of gas diffusion from taking place.

3. A mud/gas separator that pulls a vacuum on the mud should be used. The separator used in the experiments has an operating pressure of about 16 psi absolute. The separator did not yield an entirely satisfactory material balance on the gas in and out of the well. The greatest percentage of unaccounted gas was probably lost during the critical period when the mud/gas mixture was flowing out of the well. It is felt that the use of a vacuum mud/gas separator will yield a much more satisfactory material balance. Such a separator was being installed at the LSU research and training well at the time of the 1984 experiment. However, it was not ready for the author's use.

The following related topics are felt to be well suited for further study.

1. The degree to which the apparent two phase viscosity of a small bubble/mud mixture affects the rate of upward gas migration was surprising. The mechanisms thought to be responsible for this are a higher effective viscosity and greater bubble instability. Literature and/or experimental study on this topic will make experimental data from the LSU research and training well more meaningful.

2. The current study focuses on the pressure behavior of a static well that has taken a gas kick. The pressure behavior of a well circulating out a gas kick is of more practical value. The concepts of tracking the vertical distribution of gas and the gas zone elongation studied in this thesis are felt to be applicable to a pumping well also. In addition to the gas behavior, the pressure contributions from frictional losses and changing the amount of gas and mud in the system would have to be included.

BIBLIOGRAPHY

- Bourgoyne, Adam T., Jr. Personal Communication
- Brown, R. A. S.: "The Mechanics of Large Gas Bubbles in Tubes", The Canadian Journal of Chemical Eng. (October, 1965) 217-223.
- Casariago, Vicente G.: "Experimental Study of Two Phase Flow Patterns Occurring in a Well During Pressure Control Operations", MS Thesis, Louisiana State University, Baton Rouge, LA. (May, 1981)
- Davies, R. M. and Taylor, G.,: "The Mechanics of Large Bubbles Rising Through Extended Liquids and Through Liquids in Tubes". Proc. Royal Society, London (1950) 200, series A, 375-390.
- Haberman, W. L. and Morton, R. K.: "An Experimental Study of Bubbles Moving in Liquids", Trans. ASCE (1954) 227.
- Hewitt, G. F. and Roberts, D. N.: "Studies of Two Phase Flow Patterns by Simultaneous X-Ray and Flash Photography" UK Atomic Energy Authority Report AERE-M 2159 (1969).
- Ishii, T., and Pei, C. T.: "Drag Coefficient of Relatively Contaminated Gas Bubbles", The Canadian Journal of Chemical Engineering, (February, 1980), Vol. 58, 25-32.
- Koederitz, W. L.: "The Mechanics of Large Bubbles Rising in an Annulus", MS Thesis, Louisiana State University Baton Rouge, LA. (May, 1976)
- Levich, V. L., Physiochemical Hydrodynamics p. 325-326 (1962), Prentice-Hall, N.Y.
- Manevi and Mendelson: "The Rise Velocity of Bubbles in Tubes and Rectangular Channels as Predicted by Wave Theory", AIChE Journal (March, 1968) V. 14, N. 2, 295-300.
- Marrucci, G.: "Rising Velocity of a Swarm of Spherical Bubbles", Industrial Engineering Chemical Fundamentals (May, 1965), Vol. 4, No. 2, 224-225.

- Mathews, J. L.: "Upward Migration of Gas Kicks in a Shut-In Well", MS Thesis, Louisiana State University, Baton Rouge, LA. (May, 1980)
- Mendelson, H. D.: "The Prediction of Bubble Terminal Velocities from Wave Theory", AIChE Journal (March, 1967), 250-252.
- O'Brien, M. P., and Gosline, J. E.: "Velocity of Large Bubbles in Vertical Tubes", Industrial and Engineering Chemistry (December 1935) V. 27, N. 12, 1436-1440.
- Peebles, F. N., and Garber, H. J.: "Studies on the Motion of Gas Bubbles in Liquids", Chemical Engineering Progress (February, 1953), 88-97.
- Rader, Bourgoyne, and Ward: "Factors Affecting Bubble-Rise Velocity of Gas Kicks", journal of Petroleum Technology (May, 1975) 571-584.
- Rader, D. W.: "Movement of Gas Slugs Through Newtonian and Nonnewtonian Liquids in Vertical Annuli", MS Thesis, Louisiana State University, Baton Rouge, LA. (May, 1973)
- Sorour, M.M.: "Bubble Slug Transition in a Vertical Annulus", Alexandria University, Alexandria, Egypt (1982).
- Taitel, Y., Bornea, D., and Dukler, A. E.: "Modeling Flow Pattern Transitions for Upward Gas-Liquid Flow in Vertical Tubes", AIChE Journal (May, 1980) V. 26, N. 3, 345.
- Ward, R. H.: "Movement of Gas Slugs Through Static Liquids in Large Diameter Annuli", MS Thesis, Louisiana State University, Baton Rouge, LA. (August, 1974)
- Uno, S., and Kintner, R. C.: "Effect of Wall Proximity on the Rate of Rise of Single Air Bubbles in a Quiescent Liquid", A. I. Ch. Journal (September, 1956) V. 2, N. 3, 420-425.
- Zukoski, E. E. "Influence of Viscosity, Surface Tension, and Inclination Angle on Motion of Long Bubbles in Closed Tubes", Fluid Mech. (1966), Vol. 25, Part 4, 821-837.

VITA

Peter Garvey McFadden was born in West Lafayette Indiana on February 21, 1958. A two-year letterman in swimming, he graduated from E. O. Smith High School in 1976.

In the fall of 1976, he enrolled at the University of Rhode Island. In 1980 and 1981 he was employed at the Electric Boat Dry Dock and Shipbuilding Co. where he did work on Trident submarines. He received his Bachelor of Science degree in mechanical engineering from the University of Rhode Island in May 1982. He was the URI winner of the American Society of Mechanical Engineers annual paper contest. He went on to represent URI at the New England regional contest where representatives from 21 schools competed. He won that contest also.

He enrolled at Louisiana State University in the fall of 1982. He will receive his Master of Science degree in petroleum engineering in December 1984.

Mr. McFadden has accepted employment with Pennzoil Exploration and Production Co., and will begin work at the Parkersburg West Virginia office.